Inorganic Chemistry

ARTICLE

pubs.acs.org/IC

Probing Mesitylborane and Mesitylborate Ligation Within the Coordination Sphere of Cp*Ru(P^iPr_3)$^+$: A Combined Synthetic, X-ray Crystallographic, and Computational Study

Kevin D. Hesp,[†,§] Felix O. Kannemann,[†] Matthew A. Rankin,[†,∥] Robert McDonald,[‡] Michael J. Ferguson,[‡] and Mark Stradiotto*[,†]

[†]Department of Chemistry, Dalhousie University, Halifax, Nova Scotia B3H 4J3, Canada

[‡]X-ray Crystallography Laboratory, Department of Chemistry, University of Alberta, Edmonton, Alberta T6G 2G2, Canada

Supporting Information

ABSTRACT: The reaction of Cp*Ru(P^iPr_3)Cl (**1**) with $MesBH_2$ (Mes = 2,4,6-trimethylphenyl) afforded the mesitylborate complex Cp*Ru(P^iPr_3)(BH_2MesCl) (**2**, 66%). Exposure of **2** to the chloride abstracting agent $LiB(C_6F_5)_4 \cdot 2.5OEt_2$ provided $[Cp^*Ru(P^iPr_3)(BH_2Mes)]^+B(C_6F_5)_4^-$ (**3**, 54%), which features an unusual η^2-B-H monoborane ligand. The related borate complex Cp*Ru(P^iPr_3)-(BH_3Mes) (**5**, 65%) was prepared from **1** and LiH_3BMes. Attempts to effect the insertion of unsaturated organic substrates into the B−H bonds of **3** were unsuccessful, and efforts to dehydrohalogenate **2** using KO^{t}Bu instead afforded the mesitylborate complex Cp*(P^iPr_3)Ru-(BH_2MesOH) (**6**, 48%). Treatment of **1** with benzyl potassium generated an intermediate hydridoruthenium complex (**7**) resulting from dehydrogenation of a P^{i}Pr fragment, which in turn was observed to react with $MesBH_2$ to afford the mesitylborate complex Cp*($P(^iPr)_2(CH_3CCH_2)$)Ru(BH_3Mes) (**8**, 47%). Crystallographic characterization data are provided for **2**, **3**, **5**, **6**, and **8**. A combined X-ray crystallographic and density functional theory (DFT) investigation of **3** and **5**, using Natural Bond Orbital (NBO) and Atoms in Molecules (AIM) analysis, revealed that **3** and **5** are best described as donor−acceptor complexes between a Cp*(P^iPr_3)Ru$^+$ fragment and a bis(η^2-B-H) coordinating mesitylborane(borate) ligand. Significant σ-donation from the B−H bonds into the Ru^{II} center exists as evidenced by the NBO populations, bond orders, and AIM delocalization indices. In the case of **3**, the vacant p orbital on boron is stabilized by Ru→B π back-donation as well as by resonance with the mesityl group.

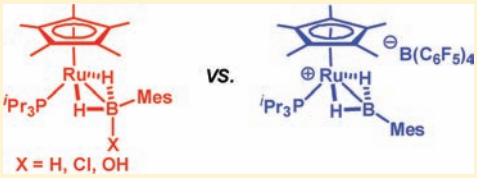

INTRODUCTION

The chemistry of transition metal complexes featuring metal−boron linkages has developed significantly in recent years, resulting in the characterization of novel metal-borane (M→BR_3), metal-boryl (M-BR_2), and metal-borylene (M═BR) species by use of spectroscopic, crystallographic, and quantum chemical techniques.[1] As part of the ongoing effort to uncover fundamentally new metal−boron bonding motifs and reactivity, and in an effort to gain mechanistic insights into prominent metal-mediated transformations including olefin hydroboration,[2] the dehydrogenative borylation of hydrocarbons,[3] and the dehydrogenation of Lewis adducts including ammonia borane,[4] there is widespread interest in documenting the bonding and reactivity behavior of B−H containing substrates within the coordination sphere of transition metals. In this context, complexes featuring monoborane (RBH_2 or R_2BH) ligands that are bound in an η^2-B-H (also denoted σ−B-H) fashion represent intriguing synthetic targets, as such species figure directly in B−H oxidative addition/reductive elimination cycles, and represent isolable models for σ−C-H species that are implicated in metal-mediated hydrocarbon C−H bond activation chemistry,[5] as well as catalytic intermediates in the dehydrogenation of amine-boranes.[4] While a relatively small number of mostly neutral η^2-B-H monoborane complexes have been prepared and characterized by use of spectroscopic, crystallographic, and computational methods,[6−9] these are few in comparison to the numerous species featuring η^2-H-H[10] or η^2-Si-H[11] ligands.[12] As such, experimental and computational investigations of new families of complexes exhibiting η^2-B-H monoborane ligation are likely to figure importantly in the continuing quest to advance our understanding of such metal−boron species.

The rich and diverse reactivity of coordinatively unsaturated cationic ruthenium complexes of the type $[Cp^*RuP_n]^+X^-$ (Cp* = η^5-C_5Me_5; n = 1, 2, or 3; X = outer-sphere anion) is well-demonstrated,[13] including reactions with organosilanes leading to isolable η^2-Si-H adducts,[11] as well as to unusual $[Cp^*(PR_3)(H)_2Ru$═$SiHR]^+X^-$ species that are generated via double geminal Si−H bond activation of $RSiH_3$.[14−16] Glaser and Tilley[14] have demonstrated that such cationic ruthenium-silylene species selectively catalyze the hydrosilylation of olefins by way of a previously undocumented mechanism involving direct addition of Ru═*Si-H* to the alkene.[17] Notably, data obtained in the course of a comparative synthetic and computational investigation of analogous neutral and cationic osmium-silylene species confirmed that the

Received: November 7, 2010
Published: February 11, 2011

Scheme 1. Synthesis of 2, 3, and 5 (Mes = 2,4,6-trimethylphenyl; $LiB(Ar^F)_4 = LiB(C_6F_5)_4 \cdot 2.5OEt_2$)

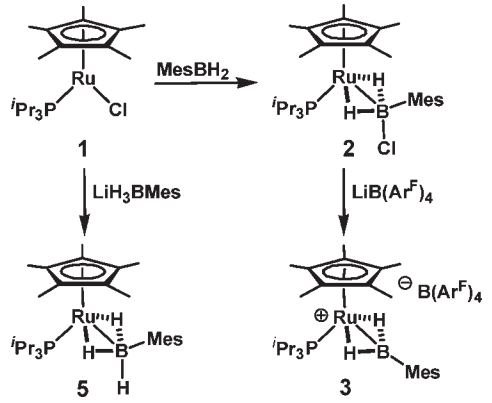

presence of a formal cationic charge on the complex is required to promote alkene insertion into the M═*Si*-*H* unit,[14,18] thereby underscoring further the significant influence of charge distribution on the chemical behavior of main group E-H fragments within the coordination sphere of reactive transition metal complexes. Intrigued by the aforementioned silane reactivity patterns, and encouraged by the diagonal relationship between silicon and boron on the periodic table, we have initiated a program focused on exploring the chemistry of primary monoboranes with 14-electron $Cp^*(PR_3)Ru^+$ fragments. We report herein on the synthesis and characterization of cationic mesitylborane ($MesBH_2$; mesityl = 2,4,6-trimethylphenyl) and neutral mesitylborate ($MesBH_2X$; X = H, Cl, OH) coordination complexes of $Cp^*(P^iPr_3)Ru^+$, including a rare example of a cationic borane complex featuring bis(η^2-B-H) ligation.[19] Also presented are the results of an X-ray crystallographic and quantum chemical investigation of $Cp^*(P^iPr_3)Ru(BH_2Mes)^+$ and $Cp^*(P^iPr_3)Ru(BH_3Mes)$ species, including a comparative analysis of the electronic structure of these complexes.

RESULTS AND DISCUSSION

Synthetic and Structural Characterization Studies. Treatment of a dark blue hexanes solution of $Cp^*Ru(P^iPr_3)Cl$ (**1**) with an equiv of $MesBH_2$ resulted in an immediate color change to dark orange; ^{31}P NMR analysis of the reaction mixture after 0.5 h revealed the quantitative formation of **2** (Scheme 1), which in turn was isolated in 66% yield. The assignment of **2** as a C_S-symmetric chloroborate complex arising from chloride transfer from ruthenium to boron is supported by NMR spectroscopic data (e.g., δ ^1H = −11.77, Ru(*H*)$_2$B; δ ^{31}P = 66.6; δ ^{11}B = 46.5, $\Delta\nu_{1/2}$ = 462 Hz), as well as single-crystal X-ray diffraction data (Figure 1). An ORTEP diagram for **2** is provided in Figure 1, while diffraction data and selected metrical parameters for each of the crystallographically characterized compounds reported herein are provided in Tables 1 and 2, respectively. While the overall connectivity within **2** can be compared with that of $Cp^*Ru(PMe_3)(BH_3Cl)$,[20] the Ru−P and Ru···B distances in **2** (2.3589(6) Å; 2.162(3) Å) are longer than those found in this comparator complex (Ru−P 2.295(1) Å); Ru···B 2.122(8) Å),[20] likely owing to the greater steric demands of the phosphine and borate ligands in **2**.[21] By comparison, no reaction was observed (^1H and ^{31}P NMR) between **1** and an equiv of either pinacolborane or catecholborane under similar experimental conditions.

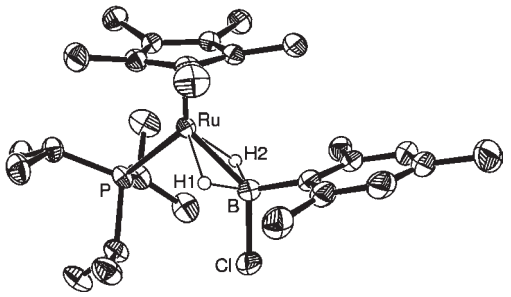

Figure 1. ORTEP diagram for **2**, shown with 50% displacement ellipsoids; selected H-atoms have been omitted for clarity.

The chloroborate complex **2** proved to be a useful synthetic precursor in the preparation of a novel cationic ruthenium species (**3**) featuring $MesBH_2$ as a ligand. When a solution of **2** in hexanes was treated with a solution of $LiB(C_6F_5)_4 \cdot 2.5OEt_2$ ($LiB(Ar^F)_4$) in fluorobenzene (Scheme 1), an immediate color change from orange to orange-yellow was observed. Monitoring the progress of the reaction by use of NMR methods revealed the consumption of **2**, along with the formation of a single new phosphorus-containing product **3** (δ ^{31}P = 72.0), which was obtained as an analytically pure solid in 54% yield upon crystallization. Integration of the ^1H NMR spectral data for pure **3** confirmed the presence of signals associated with Cp*, P^iPr_3, and Mes groups, as well as a signal in the hydride region (−10.3 ppm, 2H, $^2J_{PH}$ = 15.0 Hz) associated with this complex. As well, the broad doublet observed in the hydride region of the ^1H NMR spectrum of **3** was observed as a considerably sharper doublet in the corresponding $^1H\{^{11}B\}$ NMR spectrum, thereby suggesting the presence of some form of B···H interaction in solution. Furthermore, the solid state connectivity in **3** was determined by use of single-crystal X-ray diffraction techniques (Figure 2). A number of plausible bonding representations can be presented for **3** (Chart 1), including: the bis(η^2-B-H) structure (**3-A**); the dihydrido(borylene) formulation (**3-B**); and alternative structures featuring a formal positive charge on boron (**3-C**). However, on the basis of the crystallographic and computational (vide infra) characterization data presented herein,[22] we view **3-A** as providing the most suitable single representation of the solid state structure of **3**. In this regard, **3** can be viewed as a member of a very limited class of isolable cationic complexes featuring η^2-B-H monoborane ligation.[7,8]

Compound **3** can be described as adopting a piano-stool structure, in which the Cp^*Ru^+ fragment is supported by three neutral two-electron donors: the P^iPr_3 co-ligand as well as two dative interactions involving the bis(η^2-B-H) ligating $MesBH_2$ group, giving a formal 18 electron configuration. The unusual bis(η^2-B-H) $MesBH_2$ ligand motif featured in **3** has also been observed in $Ru(H)_2(PCy_3)_2(BH_2Mes)$ (**4**) reported by Sabo-Etienne and co-workers.[7e] While the presence of Ru−H co-ligands in the neutral complex **4** is of considerable interest in relation to σ-complex-assisted metathesis processes,[6d] the absence of such co-ligands in the novel cationic species **3** provides an opportunity to examine bis(η^2-B-H) ligation free of potential Ru−H···BH_2Mes interligand interactions. The Ru−H (1.61(3) Å and 1.60(3) Å) and B−H (1.31(3) Å and 1.28(3) Å) distances in **3** are indistinguishable from those found in the precursory complex **2**, and are in keeping with the existence of B···H interactions[23] that would appear to be inconsistent with an alternative description of **3** as the dihydridoborylene species

dx.doi.org/10.1021/ic1022328 |*Inorg. Chem.* 2011, 50, 2431–2444

Table 1. Crystallographic Data for 2, 3, 5, 6, and 8

	2	3	5	6	8
empirical formula	$C_{28}H_{49}BClPRu$	$C_{52}H_{49}B_2F_{20}PRu$	$C_{28}H_{50}BPRu$	$C_{28}H_{50}BOPRu$	$C_{28}H_{48}BPRu$
formula weight	563.97	1207.57	529.53	545.53	527.51
crystal dimensions	0.56 × 0.37 × 0.13	0.41 × 0.26 × 0.20	0.37 × 0.20 × 0.16	0.43 × 0.13 × 0.06	0.41 × 0.25 × 0.05
crystal system	monoclinic	orthorhombic	triclinic	monoclinic	triclinic
space group	$P2_1/c$	$Pbca$	$P\bar{1}$	$P2_1/c$	$P\bar{1}$
a (Å)	16.007(2)	18.8734(15)	10.4110(9)	8.3245(7)	8.5073(3)
b (Å)	10.4284(14)	18.0950(15)	12.7595(10)	17.0809(14)	17.1327(6)
c (Å)	18.504(3)	30.283(3)	21.3876(17)	20.6272(17)	19.5469(7)
α (deg)	90	90	89.6667(9)	90	84.4141(4)
β (deg)	106.1982(16)	90	85.9052(10)	101.5780(10)	86.6989(4)
γ (deg)	90	90	87.6112(10)	90	84.1438(4)
V (Å^3)	2966.1(7)	10341.9(15)	2831.4(4)	2873.3(4)	2817.42(17)
Z	4	8	4	4	4
ρ_{calcd} (g cm^{-3})	1.263	1.551	1.242	1.261	1.244
μ (mm^{-1})	0.686	0.443	0.623	0.618	0.626
range of transmission	0.9161−0.6999	0.9167−0.8394	0.9080−0.8045	0.9638−0.7769	0.9682−0.7830
2θ limit (deg)	55.00	54.96	52.80	55.00	54.96
	$-20 \le h \le 20$	$-24 \le h \le 24$	$-13 \le h \le 13$	$-10 \le h \le 10$	$-11 \le h \le 11$
	$-13 \le k \le 13$	$-23 \le k \le 23$	$-15 \le k \le 15$	$-22 \le k \le 22$	$-22 \le k \le 22$
	$-24 \le l \le 22$	$-39 \le l \le 39$	$-26 \le l \le 26$	$-26 \le l \le 26$	$-25 \le l \le 25$
total data collected	20204	86717	35486	24455	24798
independent reflections	6740	11845	35486	6553	12745
R_{int}	0.0266	0.0415	N/A	0.0421	0.0245
observed reflections	5718	9200	29614	5419	10500
data/restraints/parameters	6740/0/305	11845/0/701	35486/0/612	6553/0/306	12745/0/602
goodness-of-fit	1.063	1.047	1.029	1.032	1.027
R_1 [$F_o^2 \ge 2\sigma(F_o^2)$]	0.0302	0.0342	0.0352	0.0300	0.0301
wR_2 [$F_o^2 \ge -3\sigma(F_o^2)$]	0.0761	0.0900	0.1029	0.0771	0.0756
largest peak, hole (e Å^{-3})	0.600, −0.282	0.552, −0.347	0.746, −0.556	0.497, −0.291	0.547, −0.473

Table 2. Selected Interatomic Distances (Å) and Angles (deg) for 2, 3, 5, 6, and 8[a]

	2	3[c]	3-calc.	5[d]	5[d]	5-calc.	6	8[d,e]	8[d,e]
Ru−B	2.162(3)	1.921(2)	1.996	2.215(2)	2.210(2)	2.283	2.151(2)	2.201(3)	2.206(3)
Ru−P	2.3589(6)	2.3911(6)	2.486	2.3524(5)	2.3576(5)	2.436	2.3211(6)	2.3308(6)	2.3343(6)
Ru−H1	1.63(3)	1.61(3)	1.78	1.69(2)	1.724(17)	1.789	1.58(3)	1.69(2)	1.64(2)
Ru−H2	1.71(3)	1.60(3)	1.77	1.695(17)	1.696(19)	1.789	1.58(3)	1.70(2)	1.68(2)
B−H1	1.29(2)	1.31(3)	1.31	1.27(2)	1.281(18)	1.328	1.52(3)	1.35(2)	1.34(2)
B−H2	1.30(3)	1.28(3)	1.31	1.252(16)	1.332(19)	1.324	1.52(3)	1.31(2)	1.29(2)
B−X[b]	1.887(3)	N/A	N/A	1.117(18)	1.124(17)	1.209	1.403(3)	1.13(2)	1.14(2)
B-Cipso	1.586(3)	1.522(3)	1.516	1.597(3)	1.593(3)	1.599	1.597(3)	1.596(3)	1.598(3)
Ru−B−Cipso	123.13(16)	172.24(17)	170.34	126.93(13)	127.55(13)	124.85	120.22(15)	122.27(16)	124.91(16)
X−B−Cipso	105.83(16)	N/A	N/A	110.0(9)	110.5(9)	113.1	114.51(19)	113.6(11)	112.8(11)

[a] Data obtained from single-crystal X-ray diffraction experiments; related metrical parameters for the computationally derived structures of **3** and **5** are provided for comparison. [b] X = Cl (**2**), H3 (**5**), *O*H (**6**), and H3 (**8**). [c] P−Ru−B−C ortho torsion angles −97.6° (−103.9° calc.) and 110.5° (110.8° calc.) and the sum of the C−B−H and H−B−H angles = 356.7° (356.8° calc.) (measured in final refined structure). [d] In the two crystallographically independent molecules of **5** or **8**. [e] Within the major component of the disordered isopropenyl fragments for each of the crystallographically independent molecules of **8**: C21−C22 = 1.304(8) and 1.262(9); C21−C23 = 1.485(7) and 1.481(9).

$[Cp^*(P^iPr_3)(H)_2Ru{=}BMes]^+$ $B(C_6F_5)_4^-$ (cf. **3-B**).[24,25] The classification of **3** as a bis(η^2-B-H) monoborane complex is also in keeping with the distorted trigonal planar (sp^2-hybridized) nature of boron, as evidence by the sum of the H−B−H and H−B−C angles (ca. 357°). The coordinated $MesBH_2$ ligand in **3** features a nearly linear Ru−B−C linkage (172.24(17)° in **3**; cf. 177.1(3)° in **4**[7e]), as well as P−Ru−B−C torsion angles (97.6° and 110.5° in **3**; cf. 90.3−109.2° in **4**[7e]) that reveal a near orthogonal alignment of the B-aryl ring relative to the plane defined by ruthenium, phosphorus, and boron (Figure 2, inset). The importance of such a geometry in promoting favorable orbital overlap within the $Ru(H)_2B$ core and extending into the

dx.doi.org/10.1021/ic1022328 |*Inorg. Chem.* 2011, 50, 2431–2444

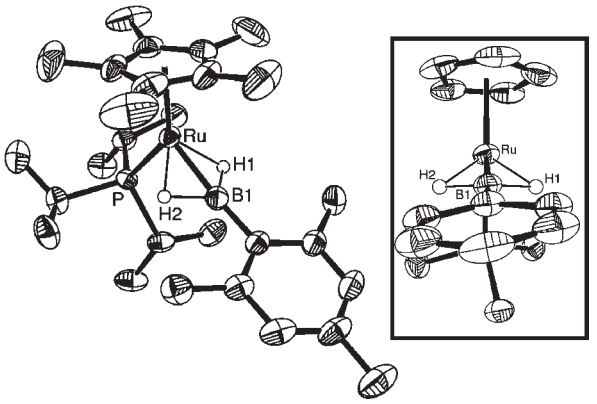

Figure 2. ORTEP diagram for **3**, shown with 50% displacement ellipsoids and with selected H-atoms and the $B(C_6F_5)_4^-$ counteranion omitted for clarity (inset: view down the Ru−B−C vector with additional C-atoms removed for clarity).

Chart 1. Three Selected Bonding Representations of 3

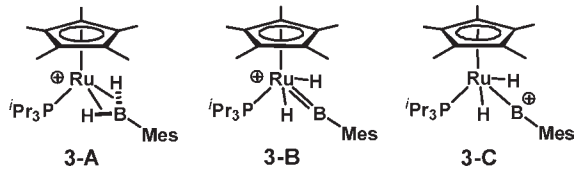

adjacent aromatic ring is discussed in the context of our computational investigation of **3** (vide infra).

The Ru···B contact (1.921(2) Å) in **3** is significantly shorter than in the chloroborate complex **2** (2.162(3) Å), and is less than the sum of the covalent radii for ruthenium and boron (ca. 2.1 Å[6]). Indeed, the Ru···B distance in **3** is shorter than almost all other crystallographically characterized complexes featuring ruthenium−boron linkages, including the η^2-B-H dialkoxyborane species $RuH_2(\eta^2\text{-}H_2)(\eta^2\text{-}BHR_2)(PCy_3)_2$ (R_2 = pinacolate, 2.173(2) Å; R_2 = catecholate, 2.124(2) Å), as well as $RuH[(\mu\text{-}H)_2Bpin](\eta^2\text{-}HBpin)(PCy_3)_2$ which contains both secondary σ-borane (2.157(5) Å) and dihydroborate (2.188(5) Å) ligands;[7f,7g] ruthenaboratranes that feature dative metal-borane (M→BR_3) interactions (ca. 2.14−2.17 Å);[26] and ruthenium-boryl complexes (ca. 2.05−2.17 Å).[27] While the Ru···B contact in **3** is statistically equal to that observed in **4** (1.938(4) Å[7e]), this distance in **3** is longer than the Ru−B distance found in a ruthenium-borylene complex (1.780(4) Å).[28] We are reluctant to interpret the relatively short Ru···B distance observed in the crystal structure of **3** as providing definitive evidence of significant covalent bonding interactions between ruthenium and boron, since it is known that the ionic contributions to bonding can be sizable in transition metal−boron complexes,[1,6] and that the coordination of two geminal η^2-E-H bonds (versus a single η^2-E-H interaction) can result in the observation of relatively short crystallographically determined Ru···E distances (E = B,[7e] Si[29]). In an effort to gain insight into the electronic structure and bonding within **3**, a comparative X-ray crystallographic/quantum chemical study involving this cationic bis(η^2-B-H) monoborane complex and the related trihydridoborate species **5** was undertaken (vide infra). Compound **5** was prepared in 65% isolated yield by treatment of $Cp^*Ru(P^iPr_3)Cl$ with LiH_3BMes (Scheme 1), and was characterized by use of spectroscopic and X-ray crystallographic techniques. The observation of distinct ^{1}H NMR signals (300 K) attributable to two equivalent bridging hydrides (−12.09 ppm) as well as a terminal B−H fragment (6.77 ppm) is consistent with the crystal structure of **5** (Figure 3). The solid state structural features of **5** mirror those of the related chloroborate **2**, with the exception that slightly longer Ru···B contacts are observed in each of the crystallographically independent molecules of **5** (2.215(2) Å and 2.210(2) Å, versus 1.921(2) Å in the cationic complex **3**). In contrast to the nearly linear Ru−B−C linkage and trigonal planar geometry observed for the coordinated bis(η^2-B-H) borane ligand in **3**, the Ru−B−C chain in each crystallographically independent molecule of **5** (126.93(13)° and 127.55(13)°) is significantly bent such that the boron center adopts a distorted tetrahedral geometry, as expected for a quaternary borate fragment.[21] No statistically significant differences in the bridging Ru−H and B−H distances (respectively) were observed within the structures of **3** and **5**.

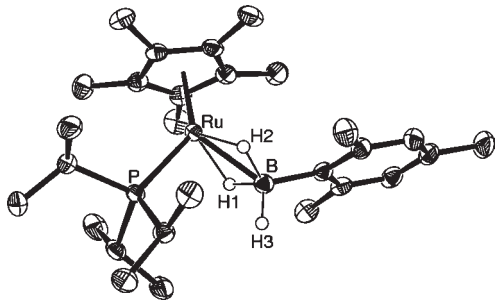

Figure 3. ORTEP diagram for one of the two crystallographically independent molecules of **5**, shown with 50% displacement ellipsoids; selected H-atoms have been omitted for clarity.

Reactivity Studies. Given the conceptual relationship between $[Cp^*(PR_3)(H)_2Ru{=}SiHR]^+X^-$ species reported by Glaser and Tilley[14] and the cationic bis(η^2-B-H) species **3**, the ability of **3** to hydroborate unsaturated substrates in a stoichiometric fashion was examined. However, no reaction was observed upon exposure of **3** to either diphenylacetylene, styrene, norbornene, or *tert*-butylethylene (1 or 10 equiv) at ambient temperature, and heating of these reaction mixtures at 50 °C afforded $^iPr_3P{\cdot}BH_2Mes$ as a major product (^{31}P NMR) after several hours. By comparison, the aforementioned cationic ruthenium-silylene complexes reported by Glaser and Tilley[14] react rapidly with α-olefins to afford isolable Si−H insertion products.

To complement the synthesis of **5** and **3**, which feature mesitylborate and mesitylborane ligation (respectively), further research efforts were directed toward preparing the related mesitylboryl complex $Cp^*(P^iPr_3)Ru(BHMes)$, which in principle could rearrange to the mesitylborylene species $Cp^*(P^iPr_3)(H)Ru{=}BMes$ via α-H elimination.[30] We initially identified the reaction of **2** with KO^tBu as a potential route to $Cp^*(P^iPr_3)Ru(BHMes)$; however, instead of effecting the dehydrohalogenation of **2**, this reaction gave rise to the mesitylborate complex $Cp^*(P^iPr_3)Ru(BH_2MesOH)$ **6** (Scheme 2), which in turn was isolated as an analytically pure solid in 48% yield. While we cannot unequivocally exclude the formation of **6** as arising from the reaction of **2** with KOH (formed in situ from KO^tBu and adventitious water), we feel that such a scenario is unlikely under the anhydrous reaction conditions employed. Instead, we view **6**

dx.doi.org/10.1021/ic1022328 |*Inorg. Chem.* 2011, 50, 2431–2444

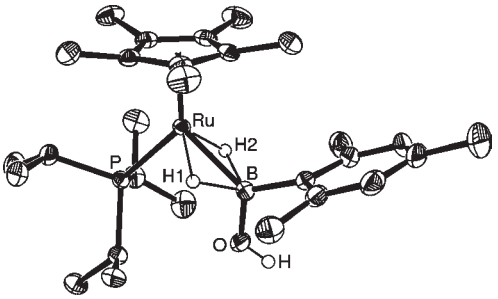

Figure 4. ORTEP diagram for **6**, shown with 50% displacement ellipsoids; selected H-atoms have been omitted for clarity.

Scheme 2. Reactivity of 2 Including the Formation of 6

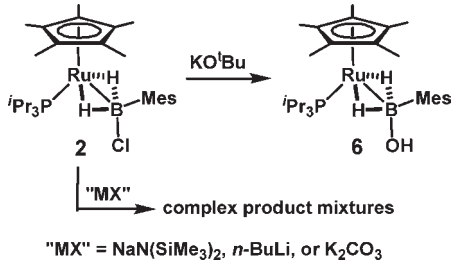

as resulting from the net elimination of 2-methylpropene in the putative reactive intermediate Cp*(P^iPr_3)Ru(BH_2MesO^tBu). The structural assignment of **6** is given on the basis of NMR spectroscopic and X-ray crystallographic data (Figure 4). The structural features of **6** mirror those observed in the related chloroborate complex **2**, and thus do no warrant further commentary. Further efforts to prepare Cp*(P^iPr_3)Ru(BHMes) via treatment of **2** with NaN($SiMe_3$)$_2$, *n*-BuLi, or K_2CO_3 generated a complex mixture of products from which no pure materials could be isolated.

The net elimination of R-H in the reaction of an alkylruthenium complex Cp*(P^iPr_3)RuR with $MesBH_2$ was identified as an alternative possible route to Cp*(P^iPr_3)Ru(BHMes). Given the utility of Cp*(P^iPr_3)OsCH_2Ph[18] as a synthetic precursor in Si−H bond activation chemistry, we sought to prepare Cp*-(P^iPr_3)RuCH_2Ph via treatment of **1** with benzyl potassium. Whereas preliminary ^{31}P NMR analysis of the reaction mixture revealed the clean conversion (in the absence of observable intermediates) to a single phosphorus-containing species (δ ^{31}P = 53.2), full characterization by use of ^{1}H and ^{13}C NMR techniques allowed for the identification of this reaction product as the hydridoruthenium complex **7** (Scheme 3). The formation of **7** can be viewed as arising from cyclometalation of an isopropyl methyl C−H fragment in the putative intermediate Cp*(P^iPr_3)RuCH_2Ph, followed by reductive elimination of toluene and β-hydride elimination.[31] Unfortunately, our attempts to isolate **7** in analytically pure form have thus far been thwarted by the apparent instability of this compound upon workup.[32] Nonetheless, **7** prepared in situ was found to react quantitatively (^{31}P NMR) with $MesBH_2$ to afford the mesitylborate complex **8**, which was obtained as an analytically pure solid in 47% yield. In contrast to the apparent C_1-symmetry observed for **7**, NMR spectroscopic data for **8** revealed a C_S-symmetric structure consistent with the presence of an uncoordinated alkenyl fragment in this complex. Furthermore, the assignment

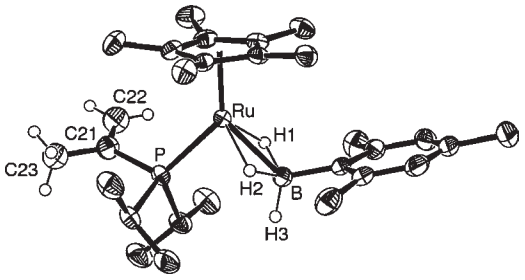

Figure 5. ORTEP diagram for one of the two crystallographically independent molecules of **8** (featuring one of the two disordered components of the isopropenyl fragment), shown with 50% displacement ellipsoids and with selected H-atoms omitted for clarity.

Scheme 3. Generation of 7 and Reaction with $MesBH_2$ to Give 8

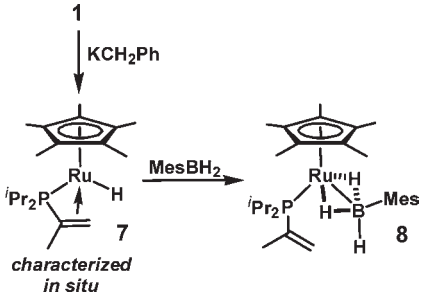

of **8** as a dehydrogenated variant of **5** is consistent with the observation of unique ^{1}H NMR (300 K) resonances attributable to two equivalent bridging hydrides (δ ^{1}H = −12.03) and a terminal B−H fragment (δ ^{1}H = 6.86), as well as data obtained by use of single-crystal X-ray diffraction techniques (Figure 5); the key metrical parameters associated with **8** compare well with those of **5**.

In keeping with the apparent inability of various unsaturated hydrocarbons to effect the clean dehydrogenation of **3** (vide supra), no reaction was observed upon exposure of **5** to norbornene or *tert*-butylethylene (1 or 10 equiv) at ambient temperature, and heating of these reaction mixtures at 90 °C led to the consumption of **5** along with the formation of an intractable mixture of phosphorus-containing products (^{31}P NMR) including **7** (ca. 10%), P^iPr_3 (ca. 40%), and an as-yet-unidentified species (ca. 30%, δ ^{31}P = 96) over the course of 48 h. The thermolysis of **8** under similar conditions was also examined in anticipation that the pendant alkene might act as a hydrogen acceptor; once again an intractable mixture of phosphorus-containing products (^{31}P NMR) was generated, including **5** (ca. 10%), **7** (ca. 5%), and an as-yet-unidentified species (ca. 70%, δ ^{31}P = 100).

Computational Approach and Geometry Optimization. In an effort to complement the X-ray crystallographic analysis of **3** and **5**, a comparative quantum chemical investigation of these complexes was conducted. Electronic structure calculations on the borane complex **3** and the borate complex **5** were performed by using the Gaussian03 package[33] using the B3LYP[34] density functional theory (DFT) method. The main group elements (C, H, B, P) were described with the 6-31G(d) basis set as implemented in Gaussian03. To improve the description of the

dx.doi.org/10.1021/ic1022328 |*Inorg. Chem.* 2011, 50, 2431–2444

B−H hydrogen atoms, the 6-31G(d,p) basis set, which includes polarization functions on H, was used for these atoms. The ruthenium center was described with the all-electron, polarized split-valence basis set of Ahlrichs and May (SVPPalls1),[35] augmented with a set of f-type polarization functions (exponent 1.2453897).[36] Cartesian basis functions (6d, 10f) are used throughout. For the electronic structure (NBO, bond order, AIM) analysis, single-point calculations on the computationally optimized geometries were performed with the same DFT method and basis sets, but including scalar relativistic effects by using the second order Douglas−Kroll−Hess (DKH) Hamiltonian.[37]

Starting from the experimental (X-ray diffraction) structures, full geometry optimizations of complexes **3** and **5** were performed. Frequency calculations on the optimized geometries characterized these structures as minimum energy points on the potential energy surface. Selected geometrical parameters of the structures optimized by use of DFT are reported in Table 2. In general, the optimized geometries are in reasonable agreement with the experimental crystal structures. The Ru−B, Ru−P, and B−H3 (in **5**) distances in the optimized structures are about 0.1 Å longer compared to the crystal structures. Such differences may be attributable to crystal packing effects absent in the computational structures, as well as to the approximate DFT method and finite basis sets used in the calculation. Also, the DFT-optimized Ru−H1 and Ru−H2 distances in the borate complex **5** are elongated by almost 0.1 Å relative to the experimentally determined structure, while for the borane complex **3** this discrepancy increases to 0.17 Å. However, the difference in the experimental Ru−H1 and Ru−H2 distances between **3** and **5** is not statistically significant because of the large standard deviations of 0.03 Å (**3**) and 0.02 Å (**5**), typical of hydrogen atoms in close proximity to a metal center. Gratifyingly, the B−H1, B−H2, and B−C_{ipso} distances, as well as the reported angles and torsion angles, are well reproduced in the computationally optimized structures.

Comparative Analysis of the Structural Parameters within 3 and 5. The neutral mesitylborate complex **5** can be viewed as a derivative of the cationic bis(η^2-B-H) monoborane species **3**, where in **5** an additional hydride ligand on the boron center contributes two electrons to the overall electron count. While quaternization of the boron center in this manner changes the hybridization state of boron from sp^2 to sp^3, it does not directly alter the first coordination sphere of ruthenium in these complexes. It is therefore interesting to compare the structural parameters around the Ru and B centers in the complexes **3** and **5**. Given the significant errors that can be associated with the X-ray crystallographic determination of hydrogen atom positions within close proximity to metal centers, analysis of the optimized structures of **3** and **5** derived from DFT calculations was undertaken.[22]

Significant differences in bond angles occur for the Ru−B−C_{ipso} angle, which changes from almost linear (172.24° expt./170.34° calc.) in **3** to strongly bent (∼127° expt./124.85° calc.) in **5**. The C_{ipso}−B−H(1,2) angles decrease from approximately trigonal planar (∼126° expt./∼121° calc.) in **3** to approximately tetrahedral (∼115° expt./∼114° calc.) in **5**. Along with the nearly tetrahedral C_{ipso}−B−H3 angle (110.3° expt./113.1° calc.) in **5**, these structural changes are in keeping with the expected change in formal hybridization from sp^2 to sp^3 on going from **3** to **5**.

Before comparing and contrasting the interatomic distances within **3** and **5**, we note that while the absolute values for interatomic distances show discrepancies of about 0.1 Å between the computational and the experimental structures, the *difference* (between complexes **3** and **5**) in these distances are in much closer agreement between calculation and experiment, having discrepancies equal to or less than 0.01 Å. The only exceptions are the Ru−H1 and Ru−H2 distances (vide supra). Interestingly, the largest change in interatomic distance occurs for the Ru···B contact, which is significantly longer (0.29 Å expt./0.29 Å calc.) in the mesitylborate complex **5** compared to cationic borane complex **3**. This indicates a much stronger Ru−B interaction in the borane complex **3**, which is further investigated in the electronic structure analysis of complexes **3** and **5** (vide infra). A similar but less dramatic increase in interatomic distance (0.07 Å expt./0.08 Å calc.) on going from **3** to **5** is found for the B−C_{ipso} bond. Conversely, the Ru−P distance contracts slightly (−0.04 Å expt./−0.05 Å calc.) from **3** to **5**, indicating that the weaker Ru−B interaction in **5** is partly compensated by a strengthening of the Ru−P bond. These changes in Ru−B and Ru−P distances between **3** and **5** are different by an order of magnitude, thereby confirming that the Ru−P interaction is much stronger than the malleable Ru···B coordination. The DFT-optimized B−H1 and B−H2 distances as well as the Ru−H1 and Ru−H2 distances in **3** and **5** are not significantly different (within 0.02 Å).

The geometrical consequences of adding a hydride ligand to the boron center in the cationic bis(η^2-B-H) monoborane complex **3**, thereby producing the neutral mesitylborate complex **5**, can be summarized as follows:

(1) The geometry of the boron center changes from trigonal planar (**3**) to tetrahedral (**5**).
(2) The Ru−B and B−C_{ipso} distances are elongated in **5** with respect to **3**, while the Ru−P bond contracts slightly.
(3) The positions of the bridging hydrogens (H1 and H2) are unaffected.

Molecular Orbital and Bond Order Analysis. To investigate the electronic structure and bonding in complexes **3** and **5**, molecular orbital (MO) and bond order analysis were performed. The canonical MOs of both systems, including the frontier orbitals, are highly delocalized and difficult to interpret. We therefore use localized MOs, in particular the Natural Bond Orbital (NBO) approach,[38] which is especially valuable in the study of donor−acceptor interactions.

In the borane complex **3**, the NBO scheme yields three lone pair orbitals on Ru (electron populations 1.91, 1.85 and 1.69) in accordance with a Ru^{II} d^6 description of this system. The P−Ru bonding orbital (pop. 1.84) has 71% contribution from P and 29% contribution from Ru, thus characterizing this interaction as predominantly dative, in contrast to a typical covalent (electron-sharing) bond. Two equivalent B−H bonding orbitals are obtained (pop. 1.61, 45% B, 55% H) for the boron center in **3**. The electron populations of the B−H bonding orbitals in **3** are noticeably smaller than in free mesitylborane (pop. 1.99, 46% B, 54% H), indicating a significant degree of σ-donation to Ru and accompanying B−H bond activation. Using second-order perturbation theory, the interaction energy of this bis(η^2-B-H) σ-donation into a formally unoccupied lone pair orbital on Ru (pop. 0.21) is estimated to be 146 kcal/mol. Thus, the NBO analysis rules out the description of **3** as a borylene complex (**3-B** or **3-C**) and confirms its nature as the bis(η^2-B-H) monoborane species **3-A**.

Finally, the formally unoccupied p orbital on B in **3** has a rather large population of 0.45 electrons, compared to a population of 0.16 in free mesitylborane. This is the result of π back-donation

from a d lone pair orbital on Ru (pop. 1.69) into the vacant p orbital on B, with an associated estimated interaction energy of 46 kcal/mol. The orbitals involved in this back-bonding are depicted in Figure 6. A comparable bonding situation involving σ-donation and π back-donation has been previously observed for the neutral mesitylborane-ruthenium complex $Ru(H)_2(PCy_3)_2(BH_2Mes)$ (**4**) reported by Sabo-Etienne and coworkers.[7e]

NBO analysis of the borate complex **5** also yields three occupied lone pair orbitals on Ru (electron populations 1.93, 1.85, and 1.82) as well as a P−Ru bonding orbital (pop. 1.91, 70% P, 30% Ru). The two σ-donating B−H bonding orbitals (pops. 1.61 and 1.62, 42% B, 58% H) have lower populations and are polarized toward the hydride fragments, compared to the third (non-donating) B−H bonding orbital (pop. 1.97, 49% B, 51% H). With second-order perturbation theory, three dominating donor(η^2-B-H)-acceptor(Ru) interactions are identified (electron populations of the different accepting Ru orbitals in parentheses): 66 kcal/mol (0.65), 67 kcal/mol (0.19), and 42 kcal/mol (0.16).

In Table 3, Wiberg bond indices[39] and overlap-weighted natural atomic orbital (NAO) bond orders[40] are presented for the Ru and B moieties in complexes **3** and **5**. These two definitions of bond order show the same characteristic changes between the cationic borane complex **3** and the neutral borate complex **5**, which also reflect the geometrical changes discussed in the previous section. Most importantly, the Ru−B bond order decreases by about 40% on going from **3** to **5** because of the absence of Ru−B π back-donation in **5** (bond lengthening of 15%). However, in both **3** and **5** the Ru−B bond order is larger than the individual Ru−H(1,2) bond orders, demonstrating the role of the B center in the bis(η^2-B-H) σ-donation to Ru. Similarly, the $B-C_{ipso}$ bond order decreases on going from **3** to **5** by about 14% because of the loss of resonance stabilization with the mesityl group in **5**, while the Ru−P and the sum of the Ru−C(Cp*) bond orders increase slightly.

The Ru−H(1,2) and B−H(1,2) bond orders are unchanged between **3** and **5**, as are the populations of the B−H bonding orbitals and the respective interatomic distances (vide supra). The sum of the Ru−H and B−H bond orders is close to unity for both bridging hydrogens, with the B−H(1,2) bond orders being about twice as large as the Ru−H(1,2) bond orders. The presence of an additional hydride ligand in the borate complex **5** has only a relatively small effect on the total bond order of the boron center because of the weakening of the Ru−B and $B-C_{ipso}$ bonds.

Finally, we compare bond orders in complexes **3** and **5** relative to the uncoordinated fragments $MesBH_2$ and $MesBH_3^-$. The geometries of the fragments were optimized with the same computational method and basis sets used for the full complexes (vide supra). As expected for bis(η^2-B-H) σ-complexes, the B−H(1,2) bond orders are significantly reduced upon complexation to Ru, by 20−40% depending on the definition of bond order. The $B-C_{ipso}$ bond order increases slightly on going from free mesitylborane to **3** because of enhanced π-electron delocalization in the presence of Ru−B π back-bonding. The B−H3 and $B-C_{ipso}$ bond orders are virtually identical in **5** and $MesBH_3^-$.

We conclude from the MO and bond order analysis that both species **3** and **5** are best described as donor−acceptor complexes between a $Cp^*(P^iPr_3)Ru^+$ fragment and a bis(η^2-B-H) coordinating mesitylborane(borate) ligand. Significant σ-donation from the B−H bonds into the Ru^{II} center exists as reflected by the NBO populations and bond orders. Complexes **3** and **5** do not show noticeable differences in the degree of B−H bond activation. The main change occurs at the B center, where the formally vacant p orbital of **3** (stabilized by π back-donation from Ru and resonance with the mesityl group) is instead replaced by a B−H σ-bond orbital in **5** with concomitant changes in geometry and electronic structure.

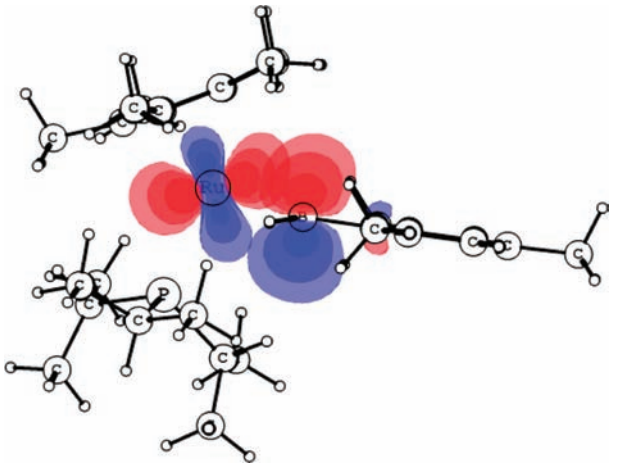

Figure 6. Orbital interactions in **3**, depicting π back-donation from a Ru valence d orbital (pop. 1.69) into the formally vacant p orbital on B (pop. 0.45). Shown are the ±0.2, ± 0.1, and ±0.05 orbital isosurfaces.

Topological Analysis of the Electron Density. Molecular Graphs. To complement the MO and bond order analysis of complexes **3** and **5**, a comparative analysis of the topology of the electron density within these complexes was conducted. To the best of our knowledge, similar computational analyses involving

Table 3. Wiberg Bond Indices and Overlap-Weighted NAO Bond Orders for the Ru and B Centers in Complexes 3 and 5

complex	bond order	Ru−P	Ru−B	Ru−H1	Ru−H2	∑ Ru−C(Cp*)	B−H1	B−H2	B−H3	$B-C_{ipso}$	B (total)
$MesBH_2$	Wiberg						0.98	0.98		1.00	3.15
3	Wiberg	0.74	0.85	0.30	0.30	1.84	0.61	0.61		1.04	3.46
5	Wiberg	0.78	0.46	0.30	0.30	1.92	0.62	0.62	0.95	0.90	3.73
$MesBH_3^-$	Wiberg						0.96	0.96	0.98	0.90	3.85
$MesBH_2$	NAO						0.83	0.83		0.96	2.69
3	NAO	0.72	0.88	0.38	0.38	1.80	0.65	0.65		1.02	3.51
5	NAO	0.76	0.58	0.39	0.39	1.85	0.64	0.65	0.82	0.87	3.74
$MesBH_3^-$	NAO						0.80	0.80	0.82	0.86	3.34

dx.doi.org/10.1021/ic1022328 |*Inorg. Chem.* 2011, 50, 2431–2444

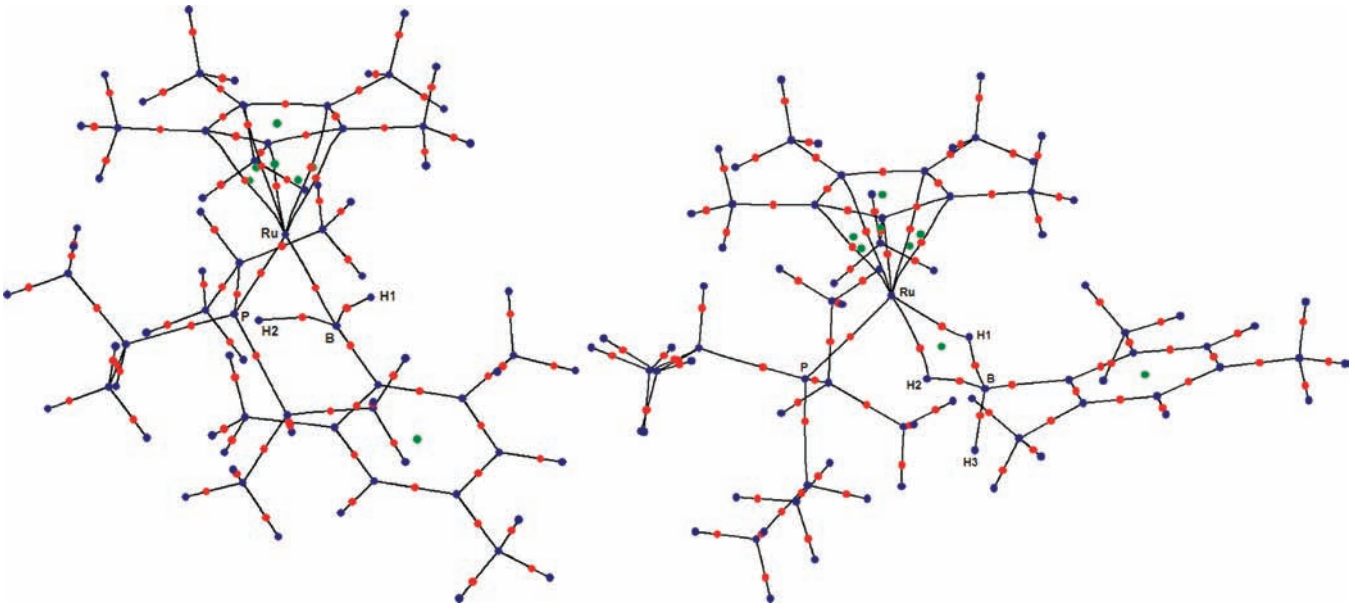

Figure 7. Molecular graphs displaying the topology of the electron density of **3** (left) and **5** (right). Shown are nuclear attractors (blue spheres), BCPs (red spheres), RCPs (green spheres), and bond paths (black lines).

4 have not been reported.[7e] While NBO analysis yields a chemically intuitive interpretation of bonding in terms of orbital interactions, the underlying quantities (localized orbitals and bond orders) are not physical observables and can lead to ambiguous interpretation. By contrast, the electron density is an observable quantity which is both routinely measured and calculated. Topological analysis of the electron density forms part of Bader's "Atoms in Molecules" (AIM) theory[41] and yields a rigorous definition of chemical bonding in terms of molecular graphs. In molecular graphs, atoms that are bonded to one another are linked by bond paths, and the point of minimum electron density along the bond path is termed bond critical point (BCP).[42] The topological analysis of the electron density of complexes **3** and **5** was carried out with the AIM2000[41c] and AIMALL[41d] programs.

Molecular graphs for complexes **3** and **5** are shown in Figure 7; for clarity, we omit bond paths and bond critical points (BCPs) between atoms on different ligands that are not covalently bonded to one another. In both complexes, the Ru center is linked to the C atoms of the Cp* ligand by five BCPs and associated bond paths, which are intersected by five ring critical points (RCPs). This topology is typical for interactions between metals and an unsaturated ring, where the electron density is delocalized over the ring perimeter instead of being confined to individual atomic sites.[41b]

Regarding the B−Ru coordination in **3** and **5**, the topology of the electron density shows remarkable differences. While the cationic borane complex **3** displays a single BCP and bond path linking the B and Ru nuclei, no such BCP exists in the neutral borate species **5**. Instead, the borate group is linked to the Ru center by bond paths emanating from the bridging hydrogens (H1 and H2). Together with the B−H(1,2) bond paths they form an almost planar four-membered ring which contains a RCP (on the line between the B and Ru nuclei). Surprisingly, no Ru−H(1,2) bond paths are found for the borane complex **3**.

We have verified that the missing Ru−H(1,2) bond paths in **3** are not an artifact of the DFT method or basis set, by performing a MP2 calculation on a smaller model complex **3s**, in which the Cp*, $MesBH_2$, and P^iPr_3 ligands of **3** were replaced by Cp, $PhBH_2$, and PH_3 groups, respectively. The geometry of this model system was optimized with B3LYP/6-31G(d,p)[main group elements]/SVPPalls1[Ru]. For the single-point MP2 calculation we employed the 6-311G(d,p) basis set for the main group atoms and an all-electron, polarized triple-ζ valence basis set (TZVPPalls2) for the Ru atom (augmented with a set of f-type polarization functions, exponent 1.2453897).[35] The topologies of the MP2 and B3LYP densities of **3s** are identical to the B3LYP density of **3**, with a single B−Ru BCP and no Ru−H(1,2) BCPs.

Inspection of Figure 7 suggests an explanation for the "missing" Ru−H(1,2) BCPs and bond paths in **3**: The ring critical point on the line between the Ru and B centers in **5** is not at the center of the four-membered Ru−H1−B−H2 ring, but in close proximity to the Ru−H(1,2) BCPs. Also, the electron density in this region is relatively flat, with density values of 0.07 e $bohr^{-3}$ at the Ru−B RCP and only 0.08 e $bohr^{-3}$ at each of the Ru−H(1,2) BCPs. Together with the bending of the Ru−H(1,2) bond paths (0.03 Å longer than the Ru−H interatomic distances), this indicates that the Ru−H(1,2) bond paths are rather unstable and susceptible to breaking because of small changes in geometry.[42]

In **3**, Ru→B π back-donation leads to a large contraction of the Ru−B interatomic distance by 0.29 Å, concomitant buildup of electron density, and formation of the Ru−B BCP (0.11 e $bohr^{-3}$). This results in the rupture of the fragile Ru−H(1,2) bond paths. Similar observations have been made for a related class of σ-complexes containing a Mn(η^2-Si-H) moiety, whereby a Mn−Si bond path present in $[Cp'Mn(CO)_2(\eta^2\text{-}HSiFPh_2)]$ is lacking in $[Cp'Mn(CO)_2(\eta^2\text{-}HSiHPh_2)]$ and disappears in the related $[CpMn(CO)_2(\eta^2\text{-}HSiCl_3)]$ complex upon increase of the Mn−Si distance by only 0.05 Å.[42,44]

The distinct molecular graphs in the Ru−H(1,2)-B region emphasize the major difference between complexes **3** and **5**, which is the existence of π back-donation in **3**, and the lack thereof in **5**. Since the topology of the electron density is very sensitive to such differences, additional AIM properties are

analyzed in the following section to provide a more complete picture of molecular structure and bonding in complexes **3** and **5**.

Topological Analysis of the Electron Density. AIM Bond Properties. In Table 4, selected AIM bond properties are presented for the Ru and B moieties in complexes **3** and **5** as well as for the fragments $Cp^*(P^iPr_3)Ru^+$, $MesBH_2$ and $MesBH_3$. Listed are the numerical values at the bond critical point for the electron density ρ_b, Laplacian of electron density $\nabla^2\rho_b$, energy density H_b, bond ellipticity ε, and delocalization index δ.[43] These AIM properties have been successfully used to characterize bonding interactions in transition metal complexes.[41b,42] In particular, the delocalization index provides a bridge between chemically intuitive bonding models and the rigorous AIM definition of bonding in terms of the topology of the electron density, as it quantifies the number of electron pairs shared between two atoms.[42] For comparison we also report values for a typical aromatic C−C bond (from the mesityl group in **3**) and a C−C single bond (from an isopropyl group in **3**).

Bond properties for the Ru−P interaction have values that are typical for dative bonding to a metal center:[41b,42] low ρ_b; small and positive Laplacian (indicating a local depletion of electron density and local excess of kinetic energy at the BCP, characteristic for closed-shell interactions); small and negative H_b; and significant delocalization index δ.[43] The values in **3**, **5**, and $Cp^*(P^iPr_3)Ru^+$ are very similar, with a slightly stronger Ru−P interaction in **5** as demonstrated by the ρ_b and δ indices.

Bond properties for the Ru−B interaction in **3** are also indicative of dative bonding. The large bond ellipticity of 0.72 indicates a strong π character,[42] demonstrating that this interaction is dominated by Ru→B π back-donation. In **5**, no Ru−B BCP exists and δ attains a low value of 0.19, indicating only a weak interaction between Ru and B.

The Ru−H(1,2) bond indices in **5** are again typical for dative interactions, in this case bis(η^2-B-H) σ-donation to the Ru^{II} center. No Ru−H(1,2) BCPs are found for the optimized geometry of **3**; however, the delocalization indices δ(Ru,H) of about 0.56 in **3** (cf. δ(Ru,H) ≈ 0.55 in **5** and δ(Mn,H) ≈ 0.63 in a series of Mn(η^2-Si-H) complexes[44]) indicate a significant sharing of electron pairs between Ru and the bridging hydrogens (i.e., significant σ-donation). Hence, the AIM delocalization indices unambiguously characterize both **3** and **5** as bis(η^2-B-H) complexes between a $Cp^*(P^iPr_3)Ru^+$ fragment and a mesitylborane(borate) ligand, thus resolving the apparent contradiction between the molecular graphs and the MO and bond order analysis (vide supra).

The B−H and B−C_{ipso} interactions are characterized as shared (covalent) interactions on the basis of their negative values of $\nabla^2\rho_b$, indicating a local concentration of electron density at the BCP. The only exception is the B−C_{ipso} bond in $MesBH_3^-$, for which the positive Laplacian suggests a strongly polar interaction. The B−H and B−C_{ipso} delocalization indices are all <1, which shows that the shared electron pair is unequally distributed between the atoms, leading to polar covalent bonds.[41b] The B−H(1,2) bonds in **3** and **5** are activated relative to the free $MesBH_2$ and $MesBH_3^-$ fragments, respectively, as shown by the decrease in electron density ($\Delta\rho_b$ = 0.03), energy density (ΔH_b = 0.04), and delocalization index ($\Delta\delta$ = 0.11 (**3**), 0.12 (**5**)) upon coordination to Ru. Conversely, the B−H3 bond in **5** is slightly strengthened relative to the free mesitylborate. The borane B−H bonds in **3** and $MesBH_2$ have noticeable ellipticities of about 0.27, which seems to indicate a π-electron delocalization from the aromatic mesityl group into the coplanar BH_2 unit. The B−C_{ipso} bond in **3** is somewhat stronger compared to **5** as evidenced by the larger ρ_b, H_b, and δ values, in agreement with the bond order analysis. Both B−C_{ipso} bond strengths increase slightly upon complexation to Ru.

An interesting pattern of variation is found for the B−C_{ipso} bond ellipticities: The ellipticity increases from $MesBH_3^-$ to $MesBH_2$ because of the trigonal planar geometry of the borane group, where the B−H bonds lead to accumulation of electron density in a plane (coplanar with the Mes group) containing the B−C_{ipso} bond. However, the ellipticity also increases from $MesBH_3^-$ to **5**, which we attribute to the weakening of the B−H1 and B−H2 bonds because of σ-donation to Ru, while the B−H3 bond is unaffected (in fact, slightly strengthened). The electron density in the B−H3 bonding orbital (perpendicular to the Mes group) is only partially canceled out by the weakened σ-donating B−H1 and B−H2 bonds (torsion angles to Mes group ±30°), leading to an accumulation of electron density in a plane perpendicular to Mes, resulting in a significant bond ellipticitiy of 0.14. In free $MesBH_3^-$, the electron densities of the 3 B−H bonds (one coplanar, two gauche to Mes) cancel out with respect to the B−C_{ipso} bond, leading to a low ellipticity of 0.03. In the borane complex **3**, the B−H(1,2) bonds accumulate electron

Table 4. AIM Bond Properties (Atomic Units) of Complexes 3 and 5[a]

interaction	complex	ρ_b[b]	$\nabla^2\rho_b$[c]	H_b[d]	ε[e]	δ[f]
Ru−P	**3**	0.07	0.14	−0.02	0.03	0.78
Ru−P	**5**	0.08	0.17	−0.02	0.21	0.84
Ru−P	$Cp^*(P^iPr_3)Ru^+$[g]	0.07	0.13	−0.02	0.23	0.73
Ru−B	**3**	**0.11**	0.12	−0.05	**0.72**	0.59
Ru−B	**5**	(**0.07**)[g]	(0.17)[g]	(−0.01)[g]	n.a.	**0.19**[h]
Ru−H1	**3**	n.a.	n.a.	n.a.	n.a.	**0.56**[h]
Ru−H2	**3**	n.a.	n.a.	n.a.	n.a.	**0.57**[h]
Ru−H1	**5**	**0.08**	0.25	−0.02	**0.50**	**0.55**
Ru−H2	**5**	**0.08**	0.25	−0.02	**0.51**	**0.54**
B−H1	**3**	0.15	−0.29	−0.15	**0.27**	0.43
B−H2	**3**	0.15	−0.28	−0.15	**0.27**	0.43
B−H[i]	$MesBH_2$	0.18	−0.27	−0.19	**0.28**	0.54
B−H1	**5**	0.12	−0.04	−0.11	0.11	0.35
B−H2	**5**	0.12	−0.04	−0.11	0.10	0.35
B−H3	**5**	0.17	−0.20	−0.18	0.09	0.50
B−H[j]	$MesBH_3^-$	0.15	−0.05	−0.15	0.02	0.47
B−C_{ipso}	**3**	0.20	−0.20	−0.22	0.04	0.65
B−C_{ipso}	$MesBH_2$	0.19	−0.10	−0.20	**0.18**	0.55
B−C_{ipso}	**5**	0.17	−0.13	−0.17	**0.14**	0.51
B−C_{ipso}	$MesBH_3^-$	0.15	**0.08**	−0.14	**0.03**	0.44
C=C(Mes)	**3**	0.32	−0.86	−0.32	0.22	1.40
C−C(iPr)	**3**	0.24	−0.52	−0.19	0.01	1.01

[a] Individual values discussed in main text are shown in bold. [b] Electron density at BCP. [c] Laplacian of electron density at BCP. [d] Energy density at BCP. [e] Bond ellipticity. [f] Electron delocalization index. [g] No Ru−B BCP in **5**, values are reported for the RCP on the line between the Ru and B centers. [h] No BCPs for Ru−B (**5**) and Ru−H(1,2) (**3**). [i] The two B−H bonds in $MesBH_2$ are equivalent by symmetry. [j] Average value of three B−H bonds in $MesBH_3^-$.

dx.doi.org/10.1021/ic1022328 |*Inorg. Chem.* 2011, 50, 2431–2444

density in a plane parallel to Mes, while π-backdonation from the Ru center leads to accumulation of electron density in a plane perpendicular to Mes. The two planes of electron density accumulation are orthogonal to each other, giving a low bond ellipticity of 0.04 despite the presence of significant π-density on the B center. This situation is similar to the triple bond in acetylene, where the two orthogonal π bonds give rise to an overall cylindrically symmetrical bond with $\varepsilon = 0$.

The results of the AIM analysis are consistent with the conclusions from the MO and bond order analysis: Both **3** and **5** are characterized as donor−acceptor complexes, where a mesitylborane(borate) ligand coordinates to a $Cp^*(P^iPr_3)Ru^+$ fragment in a bis(η^2-B-H) fashion. The covalent B−H(1,2) bonds of the ligand are activated but not broken upon coordination to the Ru center. Significant σ-donation to the metal center is indicated by the sizable δ(Ru,H) delocalization indices and the weakening of the B−H(1,2) bonds in both **3** and **5**. Ru→B π back-donation is manifested in the topology of the electron density of **3** by the existence of a Ru−B BCP with large bond ellipticity. No such interaction exists in **5**. This distinction between **3** and **5** is emphasized in the different topologies of the electron density in the Ru−H(1,2)-B region. The AIM delocalization indices and bond ellipticities are found to be extremely valuable in the characterization of Ru−P, Ru−B, and Ru−H dative bonding, as well as for investigating changes in the covalent B−H and B−C_{ipso} bonds upon coordination to Ru.

SUMMARY AND CONCLUSIONS

The synthesis of $[Cp^*Ru(P^iPr_3)(BH_2Mes)]^+B(C_6F_5)_4^-$ **3**, and its characterization by use of spectroscopic, single-crystal X-ray diffraction, and DFT computational methods, establishes this complex as a member of a very limited class of isolable cationic species featuring the unusual bis(η^2-B-H) monoborane ligation motif. In contrast to structurally related $[Cp^*(PR_3)(H)_2Ru{=}SiHR]^+X^-$ complexes,[14−16] efforts to promote the insertion of unsaturated organic substrates into the B−H bonds of **3** were unsuccessful, as were efforts to prepare the neutral mesitylboryl complex $Cp^*(P^iPr_3)Ru(BHMes)$. A comparative analysis of the solid state structure and electronic topology of **3** with **5** reveals important similarities and differences between these complexes. Both are best described as donor−acceptor complexes between a $Cp^*(P^iPr_3)Ru^+$ fragment and a bis(η^2-B-H) coordinating mesitylborane(borate) ligand, with the existence of significant σ-donation from the B−H bonds into the Ru^{II} (d^6) center confirmed by the calculated NBO populations, bond orders, and AIM delocalization indices. Additionally, in the case of **3** the vacant p orbital on boron is stabilized by π back-donation from Ru resulting in a dative Ru···B interaction, as well as by resonance with the mesityl group.

EXPERIMENTAL SECTION

General Considerations. Unless otherwise stated, all manipulations were conducted at ambient temperature in the absence of oxygen and water under an atmosphere of dinitrogen, either by use of standard Schlenk methods or within an mBraun glovebox apparatus, utilizing glassware that was oven-dried (130 °C) and evacuated while hot prior to use. Celite (Aldrich) was oven-dried for 5 d and then evacuated for 24 h prior to use. The non-deuterated solvents dichloromethane, diethyl ether, hexanes, and pentane were deoxygenated and dried by sparging with dinitrogen gas, followed by passage through a double-column solvent purification system purchased from mBraun Inc. Dichloromethane and diethyl ether were purified over two alumina-packed columns, while hexanes and pentane were purified over one alumina-packed column and one column packed with copper-Q5 reactant. Chloroform-d_1 (Aldrich) and fluorobenzene (Alfa Aesar), as well as benzene-d_6, tetrahydrofuran-d_8, methylcyclohexane-d_{14}, and bromobenzene-d_5 (Cambridge Isotopes) were degassed by using at least three repeated freeze−pump−thaw cycles and stored over 4 Å molecular sieves for 24 h prior to use. All solvents used within the glovebox were stored over activated 4 Å molecular sieves. $Cp^*Ru(P^iPr_3)Cl$ (**1**),[45] mesitylborane ($MesBH_2$),[46] and LiH_3BMes,[7e] were prepared by using literature procedures, while $LiB(C_6F_5)_4\cdot 2.5OEt_2$ ($LiB(Ar^F)_4$) was obtained from Boulder Scientific. All purchased and prepared solids were dried in vacuo prior to use. All other reagents were obtained from Aldrich (except for P^iPr_3, Strem) and were used as received. ^1H, ^{13}C, ^{11}B, and ^{31}P NMR characterization data were collected at 300 K on a Bruker AV-500 spectrometer operating at 500.1, 125.8, 160.5, and 202.5 MHz (respectively) with chemical shifts reported in parts per million downfield of $SiMe_4$ (for ^1H and ^{13}C), 85% H_3PO_4 in D_2O (for ^{31}P), or $BF_3\cdot OEt_2$ (for ^{11}B). ^1H, ^{13}C, and ^{11}B NMR chemical shift assignments are made on the basis of data obtained from ^{13}C-DEPT, ^1H-^1H COSY, ^1H-^{13}C HSQC, ^1H-^{13}C HMBC, and ^1H-^{11}B HSQC NMR experiments; NMR signals associated with $B(C_6F_5)_4^-$ are not reported. Elemental analyses were performed by Canadian Microanalytical Service Ltd., Delta, British Columbia, Canada.

Synthesis of $Cp^*Ru(P^iPr_3)(BH_2MesCl)$ (2). To a glass vial containing a magnetically stirred deep blue solution of **1** (0.059 g, 0.14 mmol) in hexanes (3 mL) was added solid $MesBH_2$ (0.018 g, 0.14 mmol) all at once. The vial was sealed with a PTFE-lined cap and magnetic stirring was initiated. Over the course of several seconds, the reaction mixture became dark orange. After 0.5 h, ^{31}P NMR data collected on an aliquot of this crude reaction mixture indicated the quantitative formation of **2**. The reaction mixture was filtered through Celite, concentrated in vacuo to about 2 mL, and stored at −37 °C. After 24 h, crystals of **2** were isolated by removal of the supernatant solution by use of a Pasteur pipet; this solution was then concentrated in vacuo to induce further crystallization. After repeating this procedure, the isolated crops of crystals were then combined and dried in vacuo, yielding **2** as an analytically pure dark orange crystalline solid (0.052 g, 0.092 mmol, 66%). Compound **2** was found to be thermally sensitive, as well as reactive toward trace air and moisture; storage under inert atmosphere at or below −37 °C is recommended. Anal. Calcd. for $C_{28}H_{49}BClPRu$: C 59.63; H 8.76; N 0.00. Found: C 59.59; H 8.71; N < 0.3. ^1H NMR (methylcyclohexane-d_{14}): δ 6.64 (s, 2H, aryl-H), 2.68 (m, 3H, $P(CHMe_2)_3$), 2.33 (s, 6H, aryl *o*-Me), 2.19 (s, 3H, aryl *p*-Me), 1.37 (s, 15H, C_5Me_5), 1.24 (d of d, $^3J_{PH}$ = 12.5 Hz, $^3J_{HH}$ = 7.5 Hz, 18H, $P(CHMe_2)_3$), −11.77 (br s, 2H, $Ru(H)_2B$); $^{13}C\{^1H\}$ NMR (methylcyclohexane-d_{14}): δ 148.3 (aryl *ipso*-quaternary), 135.2 (aryl *o*-quaternary), 133.7 (aryl *p*-quaternary), 127.3 (aryl-CH), 87.4 (C_5Me_5), 26.5 ($P(CHMe_2)_3$), 21.0 (aryl *o*-Me), 20.5 (aryl *p*-Me), 19.6 ($P(CHMe_2)_3$), 10.0 (C_5Me_5); $^{31}P\{^1H\}$ NMR (methylcyclohexane-d_{14}): δ 66.6; $^{11}B\{^1H\}$ NMR (methylcyclohexane-d_{14}): δ 46.5, $\Delta\nu_{1/2}$ = 462 Hz. Storage of a concentrated hexanes solution of **2** at −37 °C provided a suitable crystal for single-crystal X-ray diffraction studies.

Synthesis of $[Cp^*Ru(P^iPr_3)(BH_2Mes)]^+B(C_6F_5)_4^-$ (3). Compound **2** was prepared in situ by treatment of a solution of **1** (0.042 g, 0.097 mmol) in hexanes (2 mL) with solid $MesBH_2$ (0.015 g, 0.12 mmol) followed by stirring at ambient temperature, which caused a color change from blue to dark orange over the course of several seconds. After 0.25 h of magnetic stirring, a solution of $LiB(C_6F_5)_4\cdot 2.5OEt_2$ (0.084 g, 0.097 mmol) in fluorobenzene (2 mL) was added, causing a color change from dark orange to orange-yellow with the concomitant formation of a fine precipitate. After an additional 0.75 h of stirring, the precipitate was removed by filtration of the reaction mixture through Celite. The solvent and other volatiles were removed in vacuo, generating an oily yellow-orange solid that was then triturated with pentane (3 × 2 mL). Subsequent drying of the residue in vacuo afforded **3** as a yellow solid (0.084 g, 0.067 mmol,

dx.doi.org/10.1021/ic1022328 |*Inorg. Chem.* 2011, 50, 2431–2444

69%) that was determined to be about 95% pure on the basis of ^{1}H and ^{31}P NMR analysis. Analytically pure **3** was obtained as a microcrystalline yellow solid in 54% yield (based on **1**) by successive recrystallizations from concentrated diethyl ether solutions. Anal. Calcd for $C_{52}H_{49}B_2F_{20}PRu$: C 51.72; H 4.09; N 0.00. Found: C 51.55; H 4.09; N < 0.3. ^{1}H NMR (bromobenzene-d_5): δ 6.81 (s, 2H, aryl-H), 2.58 (s, 6H, aryl *o*-Me), 2.20 (s, 3H, aryl *p*-Me), 1.78 (m, 3H, P(C*H*Me$_2$)$_3$), 1.69 (d, J = 1.0 Hz, 15H, C$_5$Me$_5$), 0.97 (d of d, $^3J_{PH}$ = 14.5 Hz, $^3J_{HH}$ = 14.5 Hz, 18H, P(CH*Me*$_2$)$_3$), −10.3 (br d, $^2J_{PH}$ = 15.0 Hz, 2H, Ru(*H*)$_2$B); ^{13}C{^{1}H} NMR (bromobenzene-d_5): δ 147.3 (aryl *ipso*-quaternary), 146.9 (aryl *o*-quaternary), 130.2 (aryl *p*-quaternary), 129.7 (aryl-CH), 97.6 (*C*$_5$Me$_5$), 27.4 (d, $^1J_{PC}$ = 22.3 Hz, P(*C*HMe$_2$)$_3$), 22.1 (aryl *o*-Me), 22.0 (aryl *p*-Me), 19.7 (P(CH*Me*$_2$)$_3$), 11.2 (C$_5$*Me*$_5$); ^{31}P{^{1}H} NMR (bromobenzene-d_5): δ 72.0. We have not been able to observe ^{11}B NMR resonances for **3**, despite prolonged acquisition times using either variable temperature ^{11}B{^{1}H} NMR methods or ^{1}H-^{11}B HSQC NMR techniques, and by employing baseline correction routines. Furthermore, we have thus far not been able to obtain satisfactory IR data for **3**, possibly owing to the air-sensitivity of the complex. Storage of a dilute diethyl ether solution of **3** at ambient temperature provided a suitable crystal for single-crystal X-ray diffraction studies.

Synthesis of Cp*Ru(P^{i}Pr$_3$)(BH$_3$Mes) (5). Compound **1** was prepared in situ by treatment of a suspension of [Cp*RuCl]$_4$ (0.11 g, 0.099 mmol) in hexanes (5 mL) with ^{i}Pr$_3$P (76 μL, 0.40 mmol) followed by magnetic stirring at ambient temperature. After 0.25 h of magnetic stirring solid LiH$_3$BMes (0.083 g, 0.59 mmol) was added all at once causing a color change from deep blue to dark red with the concomitant formation of a fine precipitate. After 1 h of stirring, the reaction mixture was filtered through Celite, concentrated in vacuo to approximately 2 mL, and stored at −35 °C. After 24 h, **5** had crystallized as dark red crystals and that were isolated by removal of the supernatant solution by use of a Pasteur pipet; this solution was then concentrated in vacuo to induce further crystallization. After repeating this procedure, the isolated crops were then combined and dried in vacuo, yielding **5** as an analytically pure red crystalline solid (0.14 g, 0.26 mmol, 65%). Anal. Calcd for $C_{28}H_{50}BPRu$: C 63.46; H 9.52; N 0.00. Found: C 63.73; H 9.38; N < 0.3. ^{1}H NMR (C$_6$D$_6$): δ 7.00 (s, 2H, aryl-H), 6.77 (br s, 1H, B*H*), 2.54 (s, 6H, aryl *o*-Me), 2.41−2.28 (m, 6H, aryl *p*-Me and P(C*H*Me$_2$)$_3$), 1.43 (d, $^4J_{PH}$ = 1.3 Hz, 15H, C$_5$*Me*$_5$), 1.14 (d of d, $^3J_{PH}$ = 12.5 Hz, $^3J_{HH}$ = 7.0 Hz, 18H, P(CH*Me*$_2$)$_3$), −12.09 (br s, 2H, Ru-*H*$_2$-B); ^{13}C{^{1}H} NMR (C$_6$D$_6$): δ 135.5 (*ipso*-quaternary), 132.6 (aryl *o*-quaternary), 126.7 (aryl-*C*H), 84.5 (*C*$_5$Me$_5$), 24.2 (d, $^2J_{PC}$ = 18.6 Hz, P(*C*HMe$_2$)$_3$), 21.8 (aryl *o*-Me), 20.4 (aryl *p*-Me), 18.8 (P(CH*Me*$_2$)$_3$), 9.9 (*C*$_5$*Me*$_5$); ^{31}P{^{1}H} NMR (C$_6$D$_6$): δ 62.5; ^{11}B{^{1}H} NMR (C$_6$D$_6$): δ 41.8 ($\Delta\nu_{1/2}$ = 326.2 Hz). Storage of a concentrated pentane solution of **5** at −35 °C provided a suitable crystal for single-crystal X-ray diffraction studies.

Synthesis of Cp*Ru(P^{i}Pr$_3$)(BH$_2$MesOH) (6). Compound **2** was prepared in situ by treatment of a solution of **1** (0.10 g, 0.23 mmol) in hexanes (5 mL) with solid MesBH$_2$ (0.031 g, 0.23 mmol) followed by stirring at ambient temperature, during which time the solution turned from light blue to orange. After 0.25 h of magnetic stirring solid KO^{t}Bu (0.029 g, 0.26 mmol) was added all at once causing a color change from deep orange to yellow-red with the concomitant formation of a fine precipitate. After 3 h of stirring, the reaction mixture was filtered through Celite, concentrated in vacuo to approximately 2 mL, and stored at −37 °C. After 24 h, **6** had precipitated as fine yellow powder and was isolated by removal of the supernatant solution by use of a Pasteur pipet; this solution was then concentrated in vacuo to induce further precipitation. After repeating this procedure, the isolated crops were then combined and dried in vacuo, yielding **6** as an analytically pure yellow powder (0.059 g, 0.112 mmol, 48%). Anal. Calcd for $C_{28}H_{50}BOPRu$: C 61.60; H 9.24; N 0.00. Found: C 61.41; H 9.33; N < 0.3. ^{1}H NMR (C$_6$D$_6$): δ 6.83 (s, 2H, aryl-H), 3.74 (t, $^3J_{HH}$ = 3.0 Hz, 1H, -O*H*), 2.55 (s, 6H, aryl *o*-Me), 2.40 (m, 3H, P(C*H*Me$_2$)$_3$), 2.28 (s, 3H, aryl *p*-Me), 1.52 (s, 15H, C$_5$*Me*$_5$), 1.21 (d of d, $^3J_{PH}$ = 12.5 Hz, $^3J_{HH}$ = 7.5 Hz, 18H, P(CH*Me*$_2$)$_3$), −13.52 (br s, 2H, Ru-*H*$_2$-B); ^{13}C{^{1}H} NMR (C$_6$D$_6$): δ 147.4 (*ipso*-quaternary), 136.9 (aryl *o*-quaternary), 135.6 (aryl *p*-quaternary), 128.8 (aryl-CH), 92.1 (*C*$_5$Me$_5$), 27.9 (d, $^2J_{PC}$ = 18.9 Hz, P(*C*HMe$_2$)$_3$), 22.2 (aryl *o*-Me), 21.9 (aryl *p*-Me), 20.6 (P(C*H*Me$_2$)$_3$) 11.5 (C$_5$*Me*$_5$); ^{31}P{^{1}H} NMR (C$_6$D$_6$): δ 77.9; ^{11}B{^{1}H} NMR (C$_6$D$_6$): δ 59.7 ($\Delta\nu_{1/2}$ = 341.4 Hz). Slow evaporation of a concentrated pentane solution of **6** at ambient temperature provided a suitable crystal for single-crystal X-ray diffraction studies.

Generation and Characterization of Cp*Ru[κ^3-*P*^{i}Pr$_2$-(MeC=CH$_2$)]H (7). Compound **1** was prepared in situ by treatment of a THF-d_8 solution (2 mL) of [Cp*RuCl]$_4$ (0.012 g, 0.011 mmol) with ^{i}Pr$_3$P (8.2 μL, 0.044 mmol) followed by magnetic stirring at ambient temperature. After 0.2 h of magnetic stirring, the blue solution was quantitatively transferred via pipet to a vial containing solid benzyl potassium (0.006 g, 0.044 mmol) causing an immediate color change of the mixture to dark red. While ^{1}H and ^{31}P NMR data obtained from the reaction mixture revealed the clean conversion to **7**, attempts to isolate this compound in analytically pure form have been thwarted by its apparent instability. ^{1}H NMR (THF-d_8): δ 2.10−1.99 (m, 1H, P(C*H*Me$_a$Me$_b$)), 1.95 (s, 15H, C$_5$*Me*$_5$), 1.90−1.68 (m, 2H, P(C*H*Me$_a$Me$_b$) and MeC=C*H*$_a$H$_b$), 1.61 (d, $^3J_{PH}$ = 6.5 Hz, 3H, *Me*C=CH$_2$), 1.45 (d of d, $^3J_{PH}$ = 10.5 Hz, $^3J_{HH}$ = 7.0 Hz, 3H, P(CH*Me*$_a$Me$_b$)), 1.35 (d of d, $^3J_{PH}$ = 17.0 Hz, $^3J_{HH}$ = 7.0 Hz, 3H, P(CHMe$_a$*Me*$_b$), 1.14 (m, 1H, MeC=CH$_a$*H*$_b$), 0.89 (d of d, $^3J_{PH}$ = 19.5 Hz, $^3J_{HH}$ = 7.0 Hz, 3H, P(CH*Me*$_c$Me$_d$)), 0.76 (d of d, $^3J_{PH}$ = 14.5 Hz, $^3J_{HH}$ = 7.0 Hz, 3H, P(CHMe$_c$*Me*$_d$)), −12.31 (d, $^2J_{PH}$ = 25.0 Hz, 1H, Ru*H*); ^{13}C{^{1}H} NMR (THF-d_8): δ 91.6 (*C*$_5$Me$_5$), 37.3 (d, $^1J_{PC}$ = 21.4 Hz, MeC=CH$_2$), 28.8 (d, $^2J_{PC}$ = 13.8 Hz, MeC=*C*H$_2$), 28.3 (d, $^1J_{PC}$ = 23.9 Hz, P(*C*HMe$_a$Me$_b$), 21.6 (d, $^2J_{PC}$ = 8.8 Hz, P(CH*Me*$_c$Me$_d$), 20.8 (d, $^2J_{PC}$ = 6.3 Hz, *Me*C=CH$_2$), 19.8 (d, $^2J_{PC}$ = 7.5 Hz, P(CH*Me*$_a$Me$_b$)), 19.6 (d, $^1J_{PC}$ = 20.1 Hz, P-(CHMe$_c$*Me*$_d$)), 18.7 (P(CHMe$_c$*Me*$_d$)), 18.5 (d, $^2J_{PC}$ = 6.3 Hz, P-(CHMe$_a$*Me*$_b$)), 11.3 (C$_5$*Me*$_5$); ^{31}P{^{1}H} NMR (THF-d_8): δ 53.2.

Synthesis of Cp*Ru[κ^1-*P*^{i}Pr$_2$(MeC=CH$_2$)](BH$_3$Mes) (8). A solution of **7** (0.21 mmol) in THF (2 mL) was prepared in situ as outlined above. The reaction mixture was magnetically stirred for 0.5 h prior to the addition of solid MesBH$_2$ (0.028 g, 0.21 mmol), which caused the immediate color change to dark red-yellow. After 0.5 h, ^{31}P NMR data collected on an aliquot of this crude reaction mixture indicated the quantitative formation of **8**. The solvent was removed in vacuo affording a red-orange solid which was extracted into pentane (3 × 1 mL) followed by filtration through Celite. The combined pentane extracts were concentrated to approximately 2 mL and was stored at −37 °C. After 24 h, crystals of **8** were isolated by removal of the supernatant solution by use of a Pasteur pipet; this solution was then concentrated in vacuo to induce further crystallization. After repeating this procedure, the isolated crops of crystals were then combined and dried in vacuo, yielding **8** as an analytically pure crystalline orange-red solid (0.052 g, 0.099 mmol, 47%). Anal. Calcd for $C_{28}H_{48}BPRu$: C 63.71; H 9.17; N 0.00. Found: C 63.36; H 9.11; N < 0.3. ^{1}H NMR (C$_6$D$_6$): δ 7.00 (s, 2H, aryl-H), 6.86 (br s, 1H, B-*H*), 5.59−5.50 (m, 1H, P(MeC=C*H*$_a$H$_b$)), 5.35−5.29 (m, 1H, P(MeC=CH$_a$*H*$_b$)), 2.53 (s, 6H, aryl *o*-Me), 2.39 (s, 3H, aryl *p*-Me), 2.22 (m, 2H, P(C*H*Me$_2$)$_2$), 1.87 (m, 3H, P(*Me*C=CH$_2$)), 1.43 (d, J_{PH} = 1.3 Hz, 15H, C$_5$*Me*$_5$), 1.08 (d of d, $^3J_{PH}$ = 14.0 Hz, $^3J_{HH}$ = 7.0 Hz, 6H, P(CH*Me*$_a$Me$_b$)$_2$), 0.98 (d of d, $^3J_{PH}$ = 13.0 Hz, $^3J_{HH}$ = 7.0 Hz, 6H, P(CHMe$_a$*Me*$_b$)$_2$), −12.03 (br s, 2H, Ru-*H*$_2$-B); ^{13}C{^{1}H} NMR (C$_6$D$_6$): δ 149.3 (aryl *ipso*-quaternary), 139.4 (P(MeC=CH$_2$)), 135.4 (aryl *o*-quaternary), 132.7 (aryl *p*-quaternary), 127.3 (aryl-CH), 123.5 (d, $^2J_{PC}$ = 7.2 Hz, P(MeC=CH$_2$)), 85.0 (*C*$_5$Me$_5$), 23.8 (d, $^2J_{PC}$ = 10.3 Hz, P(*Me*C=CH$_2$)), 22.0 (d, $^1J_{PC}$ = 21.3 Hz, P(CHMe$_2$)$_2$), 21.8 (aryl *o*-Me), 20.4 (aryl *p*-Me), 17.9 (P(CH*Me*$_a$Me$_b$)$_2$), 9.6 (C$_5$*Me*$_5$); ^{31}P{^{1}H} NMR (C$_6$D$_6$): δ 66.7; ^{11}B-{^{1}H} NMR (C$_6$D$_6$): δ 43.0 ($\Delta\nu_{1/2}$ = 296.0 Hz).

Synthesis of ^{i}Pr$_3$P·BH$_2$Mes.[47] To a magnetically stirred solution of MesBH$_2$ (0.025 g, 0.19 mmol) in CH$_2$Cl$_2$ (2 mL) was added a solution of P^{i}Pr$_3$ (37 μL, 0.19 mmol) in CH$_2$Cl$_2$ (1 mL) followed by magnetic stirring; ^{31}P NMR analysis of the reaction mixture after 1 h

dx.doi.org/10.1021/ic1022328 |*Inorg. Chem.* 2011, 50, 2431–2444

indicated the quantitative formation of $^{i}Pr_3P\cdot BH_2Mes$. Removal of the solvent and other volatiles in vacuo afforded a white solid that was dissolved in pentane (3 mL) followed by filtration through Celite. Removal of the pentane afforded a microcrystalline white solid ($^{i}Pr_3P\cdot BH_2Mes$) that was determined to be >95% pure on the basis of ^{1}H and ^{31}P NMR data (0.052 g, 0.18 mmol, 95%). ^{1}H NMR ($CDCl_3$): δ 6.81 (s, 2H, aryl-H), 2.46 (s, 6H, aryl *o*-Me), 2.34 (m, 3H, $P(CHMe_2)_3$), 2.27 (d, J = 2.5 Hz, 3H, aryl *p*-Me), 2.10 (2H, BH_2), 1.27 (d of d, $^3J_{PH}$ = 12.5 Hz, $^3J_{HH}$ = 7.0 Hz, 18H, $P(CHMe_2)_3$); $^{13}C\{^1H\}$ NMR ($CDCl_3$): δ 142.0 (d, J_{PC} = 5.5 Hz, aryl *ipso*-quaternary), 133.5 (aryl *o*-quaternary), 133.4 (aryl *p*-quaternary), 127.6 (d, J_{PC} = 2.9 Hz, aryl-CH), 24.9 (aryl *o*-Me), 22.4 (d, $^1J_{PC}$ = 26.3 Hz, $P(CHMe_2)_3$), 20.9 (aryl *p*-Me), 18.0 (d, $^2J_{PC}$ = 1.4 Hz, $P(CHMe_2)_3$); $^{31}P\{^1H\}$ NMR ($CDCl_3$): δ 23.7 (br m); $^{11}B\{^1H\}$ NMR ($CDCl_3$): δ −32.1, $\Delta\nu_{1/2}$ = 130 Hz.

Crystallographic Characterization of 2, 3, 5, 6, and 8. Crystallographic data were obtained at 193(±2) K on either a Bruker PLATFORM/SMART 1000 CCD diffractometer or a Bruker D8/APEX II CCD diffractometer using a graphite-monochromated Mo Kα (λ = 0.71073 Å) radiation, employing samples that were mounted in inert oil and transferred to a cold gas stream on the diffractometer. Programs for diffractometer operation, data collection, and data reduction were supplied by Bruker. SADABS was employed as the absorption correction method for **2**, **3**, and **6**, while Gaussian integration (face-indexing) was employed for **8**. In the case of **5**, the crystal used for data collection was found to display nonmerohedral twinning, and as such TWINABS was employed as the absorption correction method. Both components of the twin were indexed with the program CELL_NOW (Bruker AXS Inc., Madison, WI, 2004). The second twin component can be related to the first component by 180° rotation about the [−0.052 1 −0.01] axis in real space and about the [0 1 0] axis in reciprocal space. Integrated intensities for the reflections from the two components were written into a SHELXL-93 HKLF 5 reflection file with the data integration program SAINT (version 7.53A), using all reflection data (exactly overlapped, partially overlapped, and non-overlapped). For each of **3**, **5**, and **6**, the structure was solved by use of direct methods, while for **2** and **8** a Patterson search/structure expansion was employed. Refinements were carried out by use of full-matrix least-squares procedures (on F^2) with R_1 based on $F_o^2 \geq 2\sigma(F_o^2)$ and wR_2 based on $F_o^2 \geq -3\sigma(F_o^2)$; for **5** and **8**, two crystallographically independent molecules were located in the asymmetric unit and refined in a satisfactory manner. Furthermore, for both crystallographically independent molecules of **8**, the isopropenyl groups were modeled successfully by employing a disordered model (60:40 ratio) featuring the interchange of the CH_2 and CH_3 positions. Anisotropic displacement parameters were employed throughout for the non-hydrogen atoms. For all structures, the non-C-*H* positions were located in the Fourier difference map and refined freely and without restraints. Otherwise, hydrogen atoms were added at calculated positions and refined by use of a riding model employing isotropic displacement parameters based on the isotropic displacement parameter of the attached atom. Additional crystallographic information is provided in the deposited CIF. All thermal ellipsoid plots were generated by use of ORTEP-3 for Windows version 1.074.[48]

■ ASSOCIATED CONTENT

Supporting Information. Single-crystal X-ray diffraction data in CIF format for **2**, **3**, **5**, **6**, and **8**, and DFT-optimized molecular structures in XYZ format for **3** and **5**. This material is available free of charge via the Internet at http://pubs.acs.org.

■ AUTHOR INFORMATION

Corresponding Author

*E-mail: mark.stradiotto@dal.ca. Fax: 1-902-494-1310. Phone: 1-902-494-7190.

Present Addresses

[§]Department of Chemistry, Yale University, New Haven, Connecticut, U.S.A.

[∥]Department of Chemistry, Massachusetts Institute of Technology, Cambridge, Massachusetts, U.S.A.

■ ACKNOWLEDGMENT

Acknowledgment is made to the Natural Sciences and Engineering Research Council (NSERC) of Canada (including a Discovery Grant for M.S., a Canada Graduate Scholarship for K.D.H., and a Postgraduate Scholarship for M.A.R.), the Canada Foundation for Innovation, the Nova Scotia Research and Innovation Trust Fund, and Dalhousie University for their generous support of this work. Computational facilities are provided by ACEnet, the regional high performance computing consortium for universities in Atlantic Canada. We also thank Drs. Michael Lumsden and Katherine Robertson of the NMR3 (Dalhousie University) for assistance in the acquisition of NMR data.

■ REFERENCES

(1) For selected reviews regarding transition metal-boron chemistry, see: (a) Braunschweig, H.; Dewhurst, R. D.; Schneider, A. *Chem. Rev.* **2010**, *110*, 3924. (b) Fontaine, F.-G.; Boudreau, J.; Thibault, M.-H. *Eur. J. Inorg. Chem.* **2008**, 5439. (c) Braunschweig, H.; Kollann, C.; Seeler, F. *Struct. Bonding (Berlin)* **2008**, *130*, 1. (d) Kays, D. L.; Aldridge, S. *Struct. Bonding (Berlin)* **2008**, *130*, 29. (e) Anderson, C. E.; Braunschweig, H.; Dewhurst, R. D. *Organometallics* **2008**, *27*, 6381. (f) Braunschweig, H.; Kollann, C.; Rais, D. *Angew. Chem., Int. Ed.* **2006**, *45*, 5254. (g) Braunschweig, H.; Rais, D. *Heteroat. Chem.* **2005**, *16*, 566. (h) Aldridge, S.; Coombs, D. L. *Coord. Chem. Rev.* **2004**, *248*, 535. (i) Braunschweig, H.; Colling, M. *Coord. Chem. Rev.* **2001**, *223*, 1. (j) Braunschweig, H. *Angew. Chem., Int. Ed.* **1998**, *37*, 1786. (k) Irvine, G. J.; Lesley, M. J. G.; Marder, T. B.; Norman, N. C.; Rice, C. R.; Robins, E. G.; Roper, W. R.; Whittell, G. R.; Wright, L. J. *Chem. Rev.* **1998**, *98*, 2685. (l) Wadepohl, H. *Angew. Chem., Int. Ed. Engl.* **1997**, *36*, 2441.

(2) (a) Crudden, C. M.; Edwards, D. *Eur. J. Org. Chem.* **2003**, 4695. (b) Beletskaya, I.; Pelter, A. *Tetrahedron* **1997**, *53*, 4957.

(3) Selected reports and reviews: (a) Mkhalid, I. A. I.; Barnard, J. H.; Marder, T. B.; Murphy, J. M.; Hartwig, J. F. *Chem. Rev.* **2010**, *110*, 890. (b) Boebel, T. A.; Hartwig, J. F. *J. Am. Chem. Soc.* **2008**, *130*, 7534. (c) Murphy, J. M.; Lawrence, J. D.; Kawamura, K.; Incarvito, C.; Hartwig, J. F. *J. Am. Chem. Soc.* **2006**, *128*, 13684. (d) Mkhalid, I. A. I.; Coventry, D. N.; Albesa-Jove, D.; Batsanov, A. S.; Howard, J. A. K.; Perutz, R. N.; Marder, T. B. *Angew. Chem., Int. Ed.* **2006**, *45*, 489. (e) Boller, T. M.; Murphy, J. M.; Hapke, M.; Ishiyama, T.; Miyaura, N.; Hartwig, J. F. *J. Am. Chem. Soc.* **2005**, *127*, 14263. (f) Hartwig, J. F.; Cook, K. S.; Hapke, M.; Incarvito, C. D.; Fan, Y.; Webster, C. E.; Hall, M. B. *J. Am. Chem. Soc.* **2005**, *127*, 2538. (g) Ishiyama, T.; Miyaura, N. *J. Organomet. Chem.* **2003**, *680*, 3.

(4) (a) Alcaraz, G.; Sabo-Etienne, S. *Angew. Chem., Int. Ed.* **2010**, *49*, 7170. (b) Staubitz, A.; Robertson., A. P. M.; Manners, I. *Chem. Rev.* **2010**, *110*, 4079. (c) Hamilton, C. W.; Baker, R. T.; Staubitz, A.; Manners, I. *Chem. Soc. Rev.* **2009**, *38*, 279. (d) Stephens, F. H.; Pons, V.; Baker, R. T. *Dalton Trans.* **2007**, 2613.

(5) For representative reviews pertaining to metal-mediated C-H bond activation, see: (a) Davies, H. M. L.; Manning, J. R. *Nature* **2008**, *451*, 417. (b) Godula, K.; Sames, D. *Science* **2006**, *312*, 67. (c) Periana, R. A.; Bhalla, G.; Tenn, W. J., III; Young, K. J. H.; Liu, X. Y.; Mironov, O.; Jones, C. J.; Ziatdinov, V. R. *J. Mol. Catal. A* **2004**, *220*, 7. (d) Crabtree, R. H. *J. Organomet. Chem.* **2004**, *689*, 4083. (e) Jones, W. D. *Acc. Chem. Res.* **2003**, *36*, 140. (f) Labinger, J. A.; Bercaw, J. E. *Nature* **2002**, *417*, 507. (g) Arndtsen, B. A.; Bergman, R. G.; Mobley, T. A.; Peterson, T. H. *Acc. Chem. Res.* **1995**, *28*, 154.

(6) For recent reviews, see: (a) Pandey, K. K. *Coord. Chem. Rev.* **2009**, *253*, 37. (b) Alcaraz, G.; Sabo-Etienne, S. *Coord. Chem. Rev.* **2008**, *252*, 2395. (c) Lin, Z. *Struct. Bonding (Berlin)* **2008**, *130*, 123. (d) Perutz, R. N.; Sabo-Etienne, S. *Angew. Chem., Int. Ed. Engl.* **2007**, *46*, 2578.

(7) For ruthenium η^2-B-H monoborane complexes, see: (a) Alcaraz, G.; Chaplin, A. B.; Stevens, C. J.; Clot, E.; Vendier, L.; Weller, A. S.; Sabo-Etienne, S. *Organometallics* **2010**, *29*, 5591. (b) Alcaraz, G.; Vendier, L.; Clot, E.; Sabo-Etienne, S. *Angew. Chem., Int. Ed.* **2010**, *49*, 918. (c) Alcaraz, G.; Grellier, M.; Sabo-Etienne, S. *Acc. Chem. Res.* **2009**, *42*, 1640. (d) Gloaguen, Y.; Alcaraz, G.; Vendier, L.; Sabo-Etienne, S. *J. Organomet. Chem.* **2009**, *694*, 2839. (e) Alcaraz, G.; Clot, E.; Helmstedt, U.; Vendier, L.; Sabo-Etienne, S. *J. Am. Chem. Soc.* **2007**, *129*, 8704. (f) Lachaize, S.; Essalah, K.; Montiel-Palma, V.; Vendier, L.; Chaudret, B.; Barthelat, J.-C.; Sabo-Etienne, S. *Organometallics* **2005**, *24*, 2935. (g) Montiel-Palma, V.; Lumbierres, M.; Donnadieu, B.; Sabo-Etienne, S.; Chaudret, B. *J. Am. Chem. Soc.* **2002**, *124*, 5624.

(8) For non-ruthenium η^2-B-H monoborane complexes, see: (a) Tang, C. Y.; Thompson, A. L.; Aldridge, S. *J. Am. Chem. Soc.* **2010**, *132*, 10578. (b) Tang, C. Y.; Thompson, A. L.; Aldridge, S. *Angew. Chem., Int. Ed.* **2010**, *49*, 921. (c) Hebden, T. J.; Denney, M. C.; Pons, V.; Piccoli, P. M. B.; Koetzle, T. F.; Schultz, A. J.; Kaminsky, W.; Goldberg, K. I.; Heinekey, D. M. *J. Am. Chem. Soc.* **2008**, *130*, 10812. (d) Crestani, M. G.; Muñoz-Hernández, M.; Arévalo, A.; Acosta-Ramírez, A.; García, J. J. *J. Am. Chem. Soc.* **2005**, *127*, 18066. (e) Schlecht, S.; Hartwig, J. F. *J. Am. Chem. Soc.* **2000**, *122*, 9435. (f) Muhoro, C. N.; He., X.; Hartwig, J. F. *J. Am. Chem. Soc.* **1999**, *121*, 5033. (g) Douglas, T. M.; Chaplin, A. B.; Weller, A. S.; Yang, X.; Hall, M. B. *J. Am. Chem. Soc.* **2009**, *131*, 15440.

(9) M(BHX) (X = OR, NR_2) complexes featuring η^2-B-H ligands have recently been reported: (a) Esteruelas, M. A.; Fernández-Alvarez, F. J.; López, A. M.; Mora, M.; Oñate, E. *J. Am. Chem. Soc.* **2010**, *132*, 5600.(b) Ref 8a herein.

(10) (a) Szymczak, N. K.; Tyler, D. R. *Coord. Chem. Rev.* **2008**, *252*, 212. (b) Heinekey, D. M.; Oldham, W. J., Jr. *Chem. Rev.* **1993**, *93*, 913. (c) Jessop, P. G.; Morris, R. H. *Coord. Chem. Rev.* **1992**, *121*, 155.

(11) (a) Lachaize, S.; Sabo-Etienne, S. *Eur. J. Inorg. Chem.* **2006**, 2115. (b) Nikonov, G. I. *Adv. Inorg. Chem.* **2005**, *53*, 217. (c) Lin, Z. *Chem. Soc. Rev.* **2002**, *31*, 239. (d) Corey, J. Y.; Braddock-Wilking, J. *Chem. Rev.* **1999**, *99*, 175.(e) Refs6b and 6d herein.

(12) (a) Kubas, G. J. *Chem. Rev.* **2007**, *107*, 4152. (b) Kubas, G. J. *Adv. Inorg. Chem.* **2004**, *56*, 127.

(13) (a) Jiménez-Tenorio, M.; Puerta, M. C.; Valerga, P. *Eur. J. Inorg. Chem.* **2004**, 17. (b) Davies, S. G.; McNally, J. P.; Smallridge, A. J. *Adv. Inorg. Chem.* **1990**, *30*, 1.

(14) Glaser, P. B.; Tilley, T. D. *J. Am. Chem. Soc.* **2003**, *125*, 13640.

(15) For reviews of transition metal-silylene chemistry, see: (a) Waterman, R.; Hayes, P. G.; Tilley, T. D. *Acc. Chem. Res.* **2007**, *40*, 712. (b) Okazaki, M.; Tobita, H.; Ogino, H. *Dalton Trans.* **2003**, 493. (c) Ogino, H. *Chem. Rec.* **2002**, *2*, 291. (d) Ogino, H.; Tobita, H. *Adv. Organomet. Chem.* **1998**, *42*, 223. (e) Zybill, C.; Handwerker, H.; Friedrich, H. *Adv. Organomet. Chem.* **1994**, *36*, 229.

(16) While crystallographically characterized $[Cp^*(PR_3)(H)_2Ru{=}SiHR]^+X^-$ complexes have yet to be reported, structurally related base-stabilized variants have appeared: Rankin, M. A.; MacLean, D. F.; Schatte, G.; McDonald, R.; Stradiotto, M. *J. Am. Chem. Soc.* **2007**, *129*, 15855.

(17) (a) Beddie, C.; Hall, M. B. *J. Phys. Chem. A* **2006**, *110*, 1416. (b) Böhme, U. *J. Organomet. Chem.* **2006**, *691*, 4400. (c) Beddie, C.; Hall, M. B. *J. Am. Chem. Soc.* **2004**, *126*, 13564.

(18) Hayes, P. G.; Beddie, C.; Hall, M. B.; Waterman, R.; Tilley, T. D. *J. Am. Chem. Soc.* **2006**, *128*, 428.

(19) A portion of this synthetic work has been communicated: Hesp, K. D.; Rankin, M. A.; McDonald, R.; Stradiotto, M. *Inorg. Chem.* **2008**, *47*, 7471.

(20) Kawano, Y.; Shimoi, M. *Chem. Lett.* **1998**, 935.

(21) Structurally diverse complexes of the type $L_nM(BH_4)$ are well-established: (a) Besora, M.; Lledós, A. *Struct. Bonding (Berlin)* **2008**, *130*, 149. (b) Xu, Z.; Lin, Z. *Coord. Chem. Rev.* **1996**, *156*, 139. (c) For $L_nM = Cp^*RuPR_3^+$ see: Suzuki, H.; Lee, D. H.; Oshima, N.; Moro-oka, Y. *Organometallics* **1987**, *6*, 1569.

(22) It has been established that the formulation of η^2-B-H monoborane complexes is best ascertained on the basis of a combined X-ray crystallographic and quantum chemical (DFT) analysis.[6b]

(23) For some other crystallographically characterized complexes featuring a Ru-H-B bridging motif, see: (a) Rankin, M. A.; MacLean, D. F.; McDonald, R.; Ferguson, M. J.; Lumsden, M. D.; Stradiotto, M. *Organometallics* **2009**, *28*, 74. (b) Rudolf, G. C.; Hamilton, A.; Orpen, A. G.; Owen, G. R. *Chem. Commun.* **2009**, 553. (c) Kawano, Y.; Hashiva, M.; Shimoi, M. *Organometallics* **2006**, *25*, 4420. (d) Saito, T.; Kuwata, S.; Ikariya, T. *Chem. Lett.* **2006**, *35*, 1224. (e) Kuan, S. L.; Leong, W. K.; Goh, L. Y.; Webster, R. D. *J. Organomet. Chem.* **2006**, *691*, 907. (f) Kuan, S. L.; Leong, W. K.; Goh, L. Y.; Webster, R. D. *Organometallics* **2005**, *24*, 4639. (g) Merle, N.; Frost, C. G.; Koicok-Köhn, G.; Willis, M. C.; Weller, A. S. *J. Organomet. Chem.* **2005**, *690*, 2829. (h) Merle, N.; Koicok-Köhn, G.; Mahon, M. F.; Frost, C. G.; Ruggerio, G. D.; Weller, A. S.; Willis, M. C. *Dalton Trans.* **2004**, 3883. (i) Foreman, M. R. St.-J.; Hill, A. F.; Owen, G. R.; White, A. J. P.; Williams, D. J. *Organometallics* **2003**, *22*, 4446. (j) Baker, R. T.; Calabrese, J. C.; Westcott, S. A.; Marder, T. B. *J. Am. Chem. Soc.* **1995**, *117*, 8777.(k) Ref 7 herein.

(24) A related cationic iron-borylene complex $[Cp^*(CO)_2Fe{=}BMes]^+X^-$ has been reported: (a) Coombs, D. L.; Aldridge, S.; Rossin, A.; Jones, C.; Willock, D. J. *Organometallics* **2004**, *23*, 2911. (b) Coombs, D. L.; Aldridge, S.; Jones, C.; Willock, D. J. *J. Am. Chem. Soc.* **2003**, *125*, 6356.

(25) By comparison, while NMR spectroscopic data for both $[Cp^*(PR_3)(H)_2Ru{=}SiHR]^+X^-$ and $[Cp^*(\mu\text{-}2\text{-}NMe_2\text{-}3\text{-}P^iPr_2\text{-indene})(H)_2Ru{=}SiHR]^+X^-$ complexes[14,16] revealed minimal Ru-H···SiHR interactions in solution, an unsymmetrical Ru-H-Si bridging motif was observed in a quantum chemical analysis of the former complexes,[17b] as well as in solid state structures of the latter base-stabilized complexes.[16]

(26) (a) Crossley, I. R.; Foreman, M. R. St.-J.; Hill, A. F.; Owen, G. R.; White, A. J. P.; Williams, D. J.; Willis, A. C. *Organometallics* **2008**, *27*, 381. (b) Hill, A. F.; Owen, G. R.; White, A. J. P.; Williams, D. J. *Angew. Chem., Int. Ed.* **1999**, *38*, 2759.

(27) (a) Rickard, C. E. F.; Roper, W. R.; Williamson, A.; Wright, L. J. *Organometallics* **2000**, *19*, 4344. (b) Braunschweig, H.; Kollann, C.; Klinkhammer, K. W. *Eur. J. Inorg. Chem.* **1999**, 1523. (c) Braunschweig, H.; Koster, M.; Wang, R. *Inorg. Chem.* **1999**, *38*, 415.

(28) Alcaraz, G.; Helmstedt, U.; Clot, E.; Vendier, L.; Sabo-Etienne, S. *J. Am. Chem. Soc.* **2008**, *130*, 12878.

(29) Atheaux, I.; Donnadieu, B.; Rodriguez, V.; Sabo-Etienne, S.; Chaudret, B.; Hussein, K.; Barthelat, J.-C. *J. Am. Chem. Soc.* **2000**, *122*, 5664.

(30) The related transformation of coordinatively unsaturated M-SiHRX species into (H)M=SiRX complexes (X = H, R) now represents an established route to metal-silylene complexes.[15a]

(31) No evidence for chemical exchange involving the alkenyl C-*H* and the Ru-*H* environments in **7** was obtained by use of ^1H-^1H EXSY NMR techniques (300 K) employing a range of mixing times.

(32) (a) While our investigations were underway, the decomposition of $Cp^*(P^iPr_3)RuCl$ in the presence of various benzylating agents leading to intractable reaction mixtures was reported: (b) Hayes, P. G.; Waterman, R.; Glaser, P. B.; Tilley, T. D. *Organometallics* **2009**, *28*, 5082. (c) The formation of the osmium analogue of **7** has been reported in the reaction of $Cp^*(P^iPr_3)OsBr$ with $KB(C_6F_5)_4$, followed by treatment with $KN(SiMe_3)_2$: Glaser, P. B.; Tilley, T. D. *Organometallics* **2004**, *23*, 5799.

(33) Frisch, M. J. et al. *Gaussian 03*, Revision E.01; Gaussian, Inc.: Wallingford, CT, 2004.

(34) (a) Becke, A. D. *Phys. Rev. A* **1988**, *38*, 3098. (b) Lee, C.; Yang, W.; Parr, R. G. *Phys. Rev. B* **1988**, *37*, 785. (c) Becke, A. D. *J. Chem. Phys.* **1993**, *98*, 5648.

(35) Ahlrichs, R.; May, K. *Phys. Chem. Chem. Phys.* **2000**, *2*, 943.

(36) This basis set was obtained from ftp://ftp.chemie.uni-karlsruhe.de/pub.

(37) (a) Douglas, M.; Kroll, N. M. *Ann. Phys.* **1974**, *82*, 89. (b) Hess, B. A. *Phys. Rev. A* **1985**, *32*, 756. (c) Hess, B. A. *Phys. Rev. A* **1986**, *33*, 3742. (d) Jansen, G.; Hess, B. A. *Phys. Rev. A* **1989**, *39*, 6016.

(38) The NBO method produces orbitals that are classified as core (CR), bonding (BD), and lone pair (LP) orbitals and are therefore directly related to the Lewis structure of the studied systems: (a) Reed, A. E.; Curtis, L. A.; Weinhold, F. *Chem. Rev.* **1988**, *88*, 899.(b) Weinhold, F.; Landis, C. R. *Valency and Bonding. A Natural Bond Orbital Donor-Acceptor Perspective*; Cambridge University Press: Cambridge, U.K., 2005.

(39) Wiberg, K. A. *Tetrahedron* **1968**, *24*, 1083.

(40) (a) Reed, A. E.; Weinhold, F. *J. Chem. Phys.* **1983**, *78*, 4066. (b) Reed, A. E.; Weinstock, R. B.; Weinhold, F. *J. Chem. Phys.* **1985**, *83*, 735.

(41) (a) Bader, R. F. W. *Atoms in Molecules: A Quantum Theory*; Oxford University Press: Oxford, U.K., 1990. (b) For the application of AIM to transition metal complexes, see: Cortes-Guzman, F.; Bader, R. F. W. *Coord. Chem. Rev.* **2005**, *249*, 633.(c) Biegler-König, F.; Schönbohm, J. *AIM2000*, Version 2.0; http://www.aim2000.de, 2002. (d) Keith, T. A., *AIMAll*, Version 09.04.23; http://aim.tkgristmill.com, 2009.

(42) Bader, R. F. W.; Matta, C. F.; Cortes-Guzman, F. *Organometallics* **2004**, *23*, 6253.

(43) Fradera, X.; Austen, M. A.; Bader, R. F. W. *J. Phys. Chem. A* **1999**, *103*, 304.

(44) McGrady, G. S.; Sirsch, P.; Chatterton, N. P.; Ostermann, A.; Gatti, C.; Altmannshofer, S.; Herz, V.; Eickerling, G.; Scherer, W. *Inorg. Chem.* **2009**, *48*, 1588.

(45) Campion, B. K.; Heyn, R. H.; Tilley, T. D. *Chem. Commun.* **1988**, 278.

(46) Smith, K.; Pelter, A.; Jin, Z. *Angew. Chem., Int. Ed.* **1994**, *33*, 851.

(47) (a) The closely related adduct $^{n}Pr_3P\cdot BH_2Mes$ has been reported: Hawthorne, M. F.; Walmsley, D. E.; Budde, W. L. *J. Am. Chem. Soc.* **1971**, *93*, 3150. (b) For other related $R_3P\cdot BH_2R'$ adducts, see: Kawano, Y.; Yamaguchi, K.; Miyake, S.; Kakizawa, T.; Shimoi, M. *Chem.—Eur. J.* **2007**, *13*, 6920.

(48) Farrugia, L. J. *J. Appl. Crystallogr.* **1997**, *30*, 565.